ARTHROPOD SYSTEMATICS & PHYLOGENY

73 (3): 351 – 384
23.12.2015

SENCKENBERG

The adult head of the annulipalpian caddisfly *Philopotamus ludificatus* McLachlan, 1878 (Philopotamidae), mouthpart homologies, and implications on the ground plan of Trichoptera

Martin Kubiak *[1a,b], Felix Beckmann[2] & Frank Friedrich[1b]

[1a] Centrum für Naturkunde (CeNak) – Zoologisches Museum, Universität Hamburg, Martin-Luther-King-Platz 3, 20146 Hamburg, Germany; Martin Kubiak * [martin.kubiak@uni-hamburg.de] — [1b] Biozentrum Grindel, Universität Hamburg, Martin-Luther-King-Platz 3, 20146 Hamburg, Germany; Frank Friedrich [frank.friedrich@uni-hamburg.de] — [2] Institut für Werkstoffforschung, Helmholtz-Zentrum Geesthacht, Außenstelle am DESY Hamburg, Notkestraße 85, 22607 Hamburg, Germany; Felix Beckmann [felix.beckmann@hzg.de] — * Corresponding author

Accepted 16.iv.2015.
Published online at www.senckenberg.de/arthropod-systematics on 14.xii.2015.

Editor in charge: Klaus-Dieter Klass.

Abstract

Adult head structures of representatives of all major trichopteran lineages were examined by using a combination of well-established morphological techniques as histology, light microscopy, scanning electron microscopy, and micro-computed tomography in combination with computer-based 3D-reconstruction. Internal and external cephalic features of the annulipalpian representative, *Philopotamus ludificatus* McLachlan, 1878, are described and illustrated in detail. The sclerites of maxilla and labium are often fused and inseparable leading to different homology hypotheses in the literature, concerning for instance the identity of the maxillary endite lobes (galea or lacinia), the composition of the basal maxillary sclerites and the origin of the haustellum. The detailed description of the skeleto-muscular system of *Philopotamus* allows for a thorough evaluation of these structures and a critical discussion of their identity. Furthermore, character complexes showing the most relevant variability among the major trichopteran lineages are presented. The ground plan conditions of the adult head in Trichoptera and Amphiesmenoptera are reconstructed for several characters. The trichopteran ground plan contains a Π-shaped tentorium with short dorsal arms, moderately sized mandibles equipped with three well-developed muscles, a small but distinct lacinia, five-segmented maxillary palps and a small haustellum. Additionally, the unusual configuration of the extrinsic dilator muscles of the salivarium is regarded as a potential autapomorphy of Trichoptera. Adult head structures observed in the annulipalpian family Philopotamidae show a remarkable number of presumably plesiomorphic features, as moderately developed and sclerotized but functionless mandibles, a small protrusible haustellum without channels on its surface, extrinsic antennal muscles originating exclusively from the tentorium, a small lacinia closely associated with the mainly membranous galea (i.e., galeolacinia), extrinsic dorsal muscles of the salivarium originating from the hypopharynx and from the premental sclerite, respectively, and small labial endite lobes.

Key words

Head morphology, skeleton, musculature, nervous system, Amphiesmenoptera, Integripalpia, Spicipalpia, Rhyacophilidae, Phryganeidae.

1. Introduction

Trichoptera (caddisflies) are comprised of two lineages, the suborder Annulipalpia (fixed-retreat makers, app. 5,500 spp.) and the suborder Integripalpia (tube-case makers, app. 5,200 spp.), plus the families Rhyacophilidae, Hydrobiosidae (both free-living), Glossosomatidae (saddle-case makers), Hydroptilidae, and Ptilocolepidae (both purse-case makers), collectively containing app. 4,000 species (Malicky 2001; Holzenthal et al. 2011).

These families have been combined in a third suborder 'Spicipalpia', or cocoon-makers, established by Weaver (1984). 'Spicipalpia' are likely not monophyletic and the taxon was not recognized in the most recent classification of the order (Holzenthal et al. 2011). The phylogenetic position of the spicipalpian families is still unresolved, and a major question in trichopteran phylogenetic research (Ross 1956; Wiggins & Wichard 1989; Schmid 1989; Ivanov 1997; Kjer et al. 2002; Holzenthal et al. 2007a,b; Malm et al. 2013). The unresolved basal branching pattern within the order also impedes the reconstruction of the trichopteran anatomical ground plan conditions. The reconstruction of the last common ancestor of the extant species is a crucial issue in phylogenetics and the necessary basis for the interpretation of evolutionary transformations in any group (see e.g., Beutel et al. 2011; Peters et al. 2014). As emphasized by Kristensen (1997), the reconstruction of the trichopteran ground plan is also impeded by the scarcity of detailed and comparative morphological and behavioral data. Especially the soft-tissue anatomy is seriously understudied for all tagmata and life stages (Friedrich & Beutel 2010; Beutel et al. 2011).

Insect head structures are a valuable source for phylogenetic information (see analyses in Beutel et al. 2011) and internal features are essential for analyzing feeding mechanisms (e.g., feeding of the mecopteran *Merope* in Friedrich et al. 2013). Anatomical data on adult cephalic structures of Trichoptera are scarce. Early investigations focused on a limited number of external features and the published data (e.g., Cummings 1914; Demoulin 1960) are largely insufficient for comparative analyses and phylogenetic evaluation. Very few studies have been devoted to internal features ('soft anatomy') of the adult head. The extensive description of *Phryganea bipunctata* (Retzius, 1783) (Integripalpia-Phryganeidae) by Crichton (1957) provides general information on cephalic features, but as this taxon is apparently deeply subordinate phylogenetically (see e.g., Malm et al. 2013), the usefulness of the data for the reconstruction of the ordinal ground plan is quite limited. The only study of a comparatively 'ancestral' trichopteran is a detailed description of the internal and external morphology of a species of *Rhyacophila* ('Spicipalpia'-Rhyacophilidae) (Klemm 1966). It was apparent that the cephalic ground plan of Trichoptera (e.g., shape and fine structure of the haustellum, musculature of the prepharynx, shape of the tentorium, etc.) could not be reliably reconstructed with the very limited data at hand.

Even though Rhyacophilidae have retained a number of apparently plesiomorphic features, a sistergroup relationship of Annulipalpia to all other trichopteran lineages ('Spicipalpia' + Integripalpia) is supported by both morphological and molecular data (Ross 1956; Frania & Wiggins 1997; Kjer et al. 2002). Malm et al. (2013) identified the spicipalpian lineages as a non-monophyletic group and as basal branches subsequently branching off, with Rhyacophilidae as the sistergroup of all the remaining Trichoptera. Like in the spicipalpian families, more or less extensive sets of potentially ancestral features also occur in Annulipalpia (Ross 1956). The 10 annulipalpian families are recently grouped into the three superfamilies Philopotamoidea (Stenopsychidae and Philopotamidae), Hydropsychoidea (Hydropsychidae), and Psychomyioidea (Kambaitipsychidae, Pseudoneureclipsidae, Psychomyiidae, Ecnomidae, Xiphocentronidae, Polycentropodidae, and Dipseudopsidae) (e.g., Holzenthal et al. 2007b; Chamorro & Holzenthal 2011; Holzenthal et al. 2011). Ross (1956) proposed Philopotamidae as sistergroup to the remaining annulipalpians based on characters of the wing venation and the two-segmented, 'primitive' male genitalia. Additionally, some of the oldest known trichopteran fossils from the Siberian Jurassic belong to this family (†*Archiphilopotamus* Sukatsheva, 1985). With about 1,000 extant species (Holzenthal et al. 2007a) Philopotamidae is also one of the most species rich families of Annulipalpia. Members of Philopotamidae are adapted to cool, running waters and are distributed worldwide (Ross 1956; Holzenthal et al. 2007a). Even though presumptive plesiomorphies (see Ross 1956) and the long evolutionary history suggests Philopotamidae as a key taxon for reconstructing the ground plan of Annulipalpia and the entire Trichoptera, the soft tissue anatomy of species of this family (and other groups of Annulipalpia) is very insufficient known and only limited information on external skeletal features is available (Ross 1956; Frania & Wiggins 1997). Consequently, we choose the philopotamid species *Philopotamus ludificatus* McLachlan, 1878 for the first comprehensive description and documentation of internal and external head structures. For the investigation of soft tissues and the skeleton of the head a combination of traditional and innovative morphological techniques was used (see Friedrich et al. 2014), including micro-computed tomography (SR-µCT), scanning electron microscopy (SEM), histological sectioning and light microscopy.

The findings are compared with own observations and literature based information on other trichopterans (e.g., Klemm 1966; Crichton 1957) and outgroup taxa (e.g., Lepidoptera – Micropterigidae; Hannemann 1956; Kristensen 2003) to discuss the homology of the mouthparts and to reconstruct the trichopteran ground plan. Additionally, character complexes potentially relevant for phylogenetic analyses are presented for further detailed investigations.

2. Material and methods

2.1. List of taxa examined and techniques applied

Annulipalpia, Philopotamidae: *Philopotamus ludificatus* McLachlan, 1878 (male, 70 % ethanol; hist., SR-µCT, SEM, diss.). **Hydropsychidae:** *Hydropsyche angustipennis* (Curtis, 1834) (male, 70 % ethanol; SR-µCT, hist., SEM).

'Spicipalpia', Rhyacophilidae: *Rhyacophila obliterata* McLachlan, 1863 (male, SR-µCT); *Rhyacophila fasciata* Hagen, 1859 (male, 70 % ethanol; SEM, diss.).

Integripalpia, Phryganeidae: *Phryganea grandis* Linnaeus, 1758 (male, 70 % ethanol; SR-µCT, SEM, diss.).

Lepidoptera (outgroup), Micropterigidae: *Micropterix calthella* (Linnaeus, 1761) (male, 70 % ethanol; hist., SEM).

[**Abbreviations:** hist. = histological section series; SR-µCT = synchrotron radiation based micro-computed tomography; SEM = scanning electron microscopy; diss. = dissection]

2.2. Morphological techniques

Synchrotron radiation based micro-computed tomography (SR-µCT). The SR-µCT data for an adult specimen of *Philopotamus* were obtained at beamline BW2 of storage ring DORIS III at the German Electron Synchrotron Facility (DESY), Hamburg (project number: I-20100317). For our studies we used a stable low photon energy beam (8 keV) and absorption contrast (for technical details of micro-tomography at beamline BW2 see Beckmann et al. 2006, 2008). Before the SR-µCT scans were carried out the appendages (wings, antennae, and legs) were cut off from the body proximally resulting in a distinctly reduced field of view. Subsequently, the specimen was dehydrated in an ethanol series and critical point dried (Balzers Critical Point Dryer) to avoid shrinking of soft tissues. The sample was mounted on a metal rod and scanned in 180° rotation (0.25° steps; 720 tomograms). The obtained image stack revealed a physical resolution of 5.68 µm (voxel size app. 2.3 µm) and allowed for easy discrimination of different tissue types. SR-µCT scans of adult specimens of *Hydropsyche*, *Rhyacophila* and *Phryganea* were also performed at the DESY facility using an identical preparations and procedures.

Computer-based 3D-reconstruction. A combination of different software packages (Visage Imaging Amira® 5.4, Bitplane Imaris 6, and Autodesk® Maya 2014) was applied to reconstruct the head morphology of *Philopotamus* based on µCT image data three-dimensionally. Amira software in combination with a Wacom Cintiq 22HD interactive pen display was used for segmentation of raw image data. Due to high density resolution of the SR-µCT scan different types of soft tissue such as muscles, glands, nerves, and also the sclerotization of the skeleton could be easily distinguished. An image stack series was obtained for each segmented structure and subsequently transferred into Bitplane Imaris 6 software for automatic creation of surface objects. Subsequently, for final post processing in Maya 2014 software all surface files (.iv) were converted into object files (.obj) using Transform2 64 bit software (Heiko Stark, Jena, Germany; URL: http://starkrats.de). The modeling of minor surface artifacts, reduction of file size, and surface renderings were processed in Maya 2014 software (for details see Friedrich et al. 2013).

Histology. Heads of *Philopotamus* and *Hydropsyche* were embedded in Araldite resin and cut at 1 µm with a Microm Microtome (HM 360) with diamond knife. The obtained cross section series were stained with toluidin blue and fuchsin. Digitalization was carried out using a Leica DM6000 microscope with slide scanning option (based on MetaMorph software). The photographed sections were automatically aligned and processed using Visage Imaging Amira 5.4® software.

Light microscopy imaging. Light microscopy imaging represents a useful tool for the documentation of coloration pattern and allows for easy discrimination of membranous and well-sclerotized areas of the insect body. The head of a male of *Philopotamus* was dehydrated in an ethanol series and critical point dried (Balzers Critical Point Dryer). Subsequently, it was glued on a small insect pin for imaging in standard morphological views. Photographs were taken using a Passport II system built by Visionary Digital™, equipped with a Canon EOS 6D digital camera and a 65 mm Canon compact macro-lens. Helicon Focus Pro X64 was used to combine the partially focused images.

Scanning electron microscopy (SEM). The fine structure of the external head capsule and its appendages was studied and documented by using SEM imaging. The head of a male of *Philopotamus* was dehydrated in an ethanol series, critical point dried (Balzers Critical Point Dryer), glued on a pin, and finally fixed to a specimen holder following the methods of Pohl (2010). The sample was evenly coated with platinum using a Polaron SC7650 Sputter Coater. SEM images were taken with a LEO 1525 scanning electron microscope at 5 or 10 keV.

Terminology. The terminology of the skeleton is mainly based on Snodgrass (1935) and Beutel et al. (2014). Sensilla are named and homologized after Melnitsky & Ivanov (2011). The names of muscles are designated by the areas of their origin and insertion sites (abbreviations used in the text: O = origin, I = insertion). If this alone is ambiguous, the topographical orientation (e.g., ventralis vs. dorsalis, etc.) is added. They are homologized with the terminologies used by Hannemann (1956), v. Kéler (1955), and Wipfler et al. (2011) (see Table 1). The musculature of other trichopteran species investigated in the present study or taken from the literature (Crichton 1957; Klemm 1966) is also summarized in Table 1.

The systematics follows Holzenthal et al. (2011). Nomenclature for Trichoptera taxa is adopted from Malicky (2005).

Fig. 1. *Philopotamus ludificatus* McLachlan, 1878: head, light-microscopic images, anterior view. — ***Abbreviations***: acl(d) – distal part of anteclypeolabrum, acl(p) – proximal part of anteclypeolabrum, as – antennal socket, atf – antennifer, atp – anterior tentorial pit, cpe – compound eye, cs – coronal sulcus, fcsw – frontoclypeal setal wart, fgs – frontogenal sulcus, fl – flagellomere, fo – fossa of subgenal process, fpc – frontopostclypeus, fs – frontal sulcus, fsw – frontal setal wart, ge – gena, gp – subgenal process, hf – horizontal furrow between frontopostclypeus and anteclypeolabrum, hst – haustellum, ias – interantennal sulcus, lap – labial palp, loc – lateral ocellus, md(m) – membranous part of mandible, md(s) – mandibular sclerite, moc – median ocellus, mxp – maxillary palp, ped – pedicellus, pfs – postfrontal sulcus, sca – scapus, srts – smooth ribbed trichoid sensillum, ve – vertex, vsw(a) – anterior setal wart of vertex, vsw(p) – posterior setal wart of vertex, I–V – number of palpomere. (Scale bar: 250 µm)

3. Results

3.1. General appearance

The mean body length of adults of *P. ludificatus* is 8.2 mm (6.2–10.2 mm; n = 25) for males and 9.9 mm (8.0–11.7 mm; n = 25) for females. The body color of the adults is dark brown. The ovate forewings are brown with large, evenly distributed yellowish to ochre spots. The hindwings are uniformly light brown. The wings are held roof-like folded above the abdomen when the living insect is at rest. Large parts of the body and especially the forewings have a dense vestiture of setae and microtrichia. The tibia of all three pairs of legs bear large, ochre spurs (spur formula 2,4,4).

3.2. Head capsule

The head is orthognathous and largely covered by a dense vestiture of minute microtrichia (Fig. 6A,B). The margin

Fig. 2. *Philopotamus ludificatus* McLachlan, 1878: head, light-microscopic images. **A**: lateral view, **B**: posterior view. — ***Abbreviations***: acl(d) – distal part of anteclypeolabrum, acl(p) – proximal part of anteclypeolabrum, bst – basistipes, cd – cardo, cpe – compound eye, cvm – cervical membrane, dst – dististipes, eph – epipharynx, fl – flagellomere, fsw – frontal setal wart, ge – gena, gp – subgenal process, hss – hypostomal sulcus, hst – haustellum, laf – semicircular fold of labium, lal – labial lobe, lap – labial palp, lapl – central plate of labium, loc – lateral ocellus, md(s) – mandibular sclerite, mxp – maxillary palp, occ – occiput, ocs – occipital sulcus, ped – pedicellus, pge – postgena, pocc – postocciput, ppg – palpiger, pss – pleurostomal sulcus, sca – scapus, ts – temporal sulcus, tsi – triangular membranous incision of stipes, tss – transstipital sulcus, ve – vertex, vsw(p) – posterior setal wart of vertex, wpge – wing-shaped extension of postgena, I–V – number of palpomere. (Scale bars: 250 µm)

of the antennal foramen is slightly reinforced by the circumantennal sulcus[1] ('antennal socket' sensu Snodgrass 1935, as in Fig. 1). The antennal socket is ventrally suspended by a large extension (antennifer, atf in Figs. 1, 6A) which is continuous with the dorsal end of the strong frontogenal sulcus (fgs in Fig. 1), interconnecting the ventral margin of the antennal socket and the base of the anterior tentorial arm (= anterior tentorial pit, atp in Figs. 1, 6A). The frontal sulci (fs) diverge anteriorly from the median coronal sulcus (cs) directly behind the median ocellus (Fig. 1). They run ventrolaterad in a straight line toward the antennal socket (obliterated at level of the frontal setal warts [fsw in Fig. 1]; see below). The coronal sulcus extends backwards toward the occipital foramen. The dorsal part of the head capsule represents the vertex (ve in Fig. 1). It is not distinctly bordered laterally, but continuous with the gena (ge in Fig. 2A) and the occiput (occ in Fig. 12B). Halfway between the lateral ocelli and the occiput a postfrontal sulcus (pfs in Fig. 1) arises from the coronal sulcus, runs laterad of the lateral ocellus anteriorly and meets the antennal socket dorsally.

[1] The term 'sulcus' refers to any line of cuticular inflection forming internal ridges. In contrast, the term 'suture' is only used for unsclerotized lines between two adjacent sclerotized areas, which are not present in the adult head capsule of caddisflies (see Snodgrass 1963: 9; Kristensen 2003: 39).

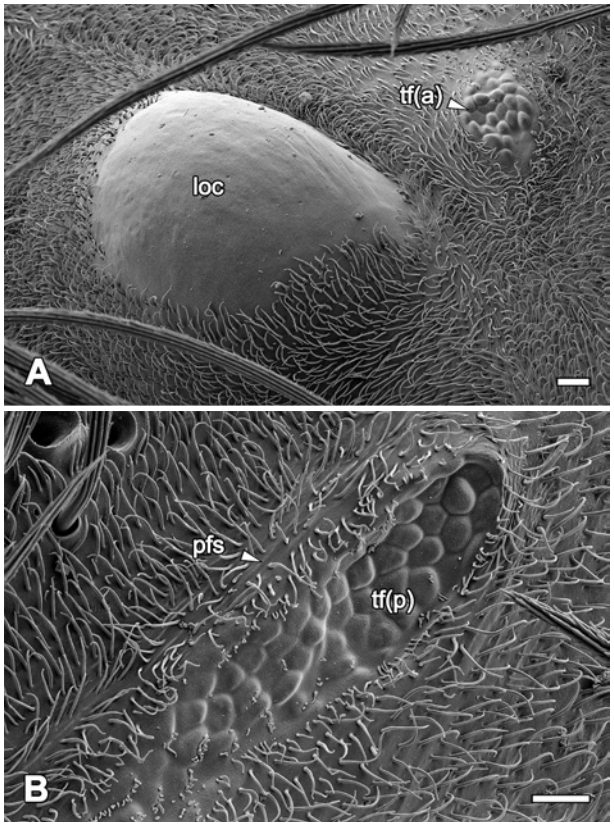

Fig. 3. *Philopotamus ludificatus* McLachlan, 1878: details of head capsule, SEM images. **A**: dorsal view on lateral ocellus with adjacent tubercular field (tubercular field marked by arrow head), **B**: detail of tubercular field behind the postfrontal sulcus (postfrontal sulcus marked by arrow head). — ***Abbreviations***: loc – lateral ocellus, pfs – postfrontal sulcus, tf(a) – anterior tubercular field of vertex, tf(p) – posterior tubercular field of vertex. (Scale bars: 10 µm)

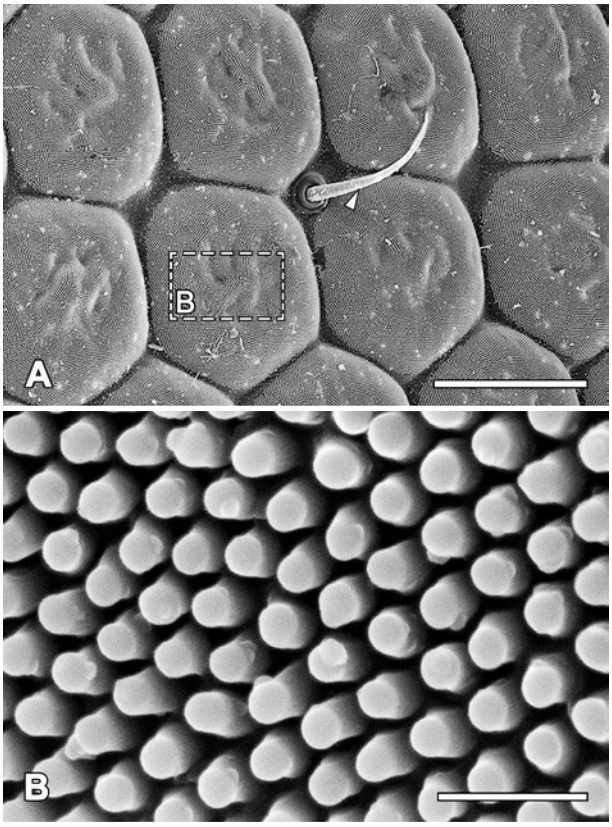

Fig. 4. *Philopotamus ludificatus* McLachlan, 1878: details of compound eye, SEM images. **A**: ommatidia with interommatidial sensillum (marked by arrow head), **B**: ultrastructure of ommatidial surface with corneal nipples. (Scale bars: A: 5 µm; B: 300 nm)

Below the median ocellus a very distinct, curved interantennal sulcus (ias in Fig. 1) runs ventrolaterad toward the frontoclypeal setal wart (see below) (Fig. 1).

The triangular facial area dorsally and laterally delimited, respectively, by the frontal sulcus and the frontogenal sulcus is a frontopostclypeus without any external demarcation of a frontoclypeal boundary (i.e., epistomal sulcus) (Fig. 1); the area above a line connecting the anterior tentorial pits bears a smooth median depression.

The lower facial region is subdivided into ante- and postclypeus by a conspicuous horizontal furrow (hf in Figs. 1, 12A); the head capsule areas adjacent to the latter are less pigmented than elsewhere, and since muscle origins indicate their clypeal nature and the apical (/ventral) area must include a labral component, they can conveniently be termed postclypeus (i.e., frontopostclypeus, fpc in Fig. 1) and anteclypeolabrum (acl(p)/acl(d) in Fig. 1), respectively. The upper/dorsal part (acl(p)) of the anteclypeolabrum has a sparse vestiture of strong smooth ribbed trichoid sensilla and a few placoid sensilla (Fig. 7A), while the lower/apical part (acl(d)) is weakly sclerotized and pigmented (Fig. 1).

The lateral parts of the head capsule, enclosing the compound eyes, are formed by the genae (ge in Fig. 2A). The gena bears a row of five strong dentate and ribbed trichoid sensilla behind the compound eye (Fig. 2A,B). Three basiconic sensilla (bs in Fig. 6A) are located on its anterior surface between the frontogenal sulcus and the anterior margin of the compound eye. Posteriorly, the gena is delimited from the postgenal region by an incomplete occipital sulcus (ocs in Fig. 2A,B). This sulcus dissappears dorsally (behind the compound eye) but ventrally splits into an anterior pleurostomal sulcus (pss) and a posterior hypostomal sulcus (hss) (both in Fig. 2A,B). The two latter sulci demarcate the dorsal margin of the small subgena, which forms a strong, heavily sclerotized process lateral to the base of the mandible. The subgenal process (gp in Figs. 1, 2A,B) is enforced by a strong sulcus and bears an oval fossa (fo in Fig. 1) apically. This structure forms the articular surface of the posterior joint of the pupal mandible.

The posteroventral parts of the head capsule are formed by the postgenae (pge in Fig. 2A,B), which are dorsally delimited from the occiput/postocciput by a strong sulcus ('sulcus temporalis' sensu KLEMM 1966, ts in Fig. 2A). The mesal halves of the postgenae are bent posterad and form wing-shaped extensions (wpge in Fig. 2B) connected with the extensive cervical membrane (cvm in Fig. 2B). A ventral closure of the head capsule (e.g., postgenal bridge, gula) is absent (Fig. 2B). Occipital and postoccipital regions are inseparable. Dorsolat-

eral to the tentorial bridge a prominent process forming the median margin of the postoccipital component of the composite occipital and postoccipital region ('condylus occipitalis' sensu Snodgrass 1935, cocc in Fig. 12B) is developed on each side of the occipital foramen, articulating with the lateral cervical sclerite.

The foramen occipitale is divided by the tentorial bridge into a broad, trapezoid upper part (app. ⅔ of the opening) and a smaller lower part (app. ⅓ of the opening). The lower opening has the margins reinforced by a strong sulcus laterally, but is ventrally just closed by the cervical membrane (Fig. 12B).

The head capsule bears a vestiture of strong dentate ribbed trichoid sensilla densely clustered on bulged setal warts (after Oláh & Johanson 2007). One slightly raised frontoclypeal setal wart (fcsw in Figs. 1, 6A) is located on the lateral frontopostclypeal region (fpc in Fig. 1) between the anterior tentorial pit and the antennal socket (Fig. 6A). Three closely adjacent setal warts (two lateral and one median) are arranged in a broad w-shaped pattern in the frontal region (= frontal setal wart, fsw in Figs. 1, 6A) bordered anteriorly by the median ocellus, laterally by the postfrontal sulcus and posteriorly by the frontal sulcus and the lateral ocelli. A pair of large triangular setal warts (= anterior setal wart of vertex, vsw(a) in Fig. 1) is located on the vertex between the lateral ocelli and the meeting point of coronal sulcus and postfrontal sulcus. The posterolateral regions of the vertex bear extremely large, strongly bulged setal warts (= posterior setal wart of vertex, vsw(p) in Figs. 2A, 12B). These areas are posteriorly reinforced by strong internal sulci at their anterior and lateral margins. A shallow furrow (tf(p) in Fig. 3B) is located directly behind the dorsal setal wart of the vertex. Its surface is tubercular and bare of microtrichia. A similarly structured but slightly bulged field (tf(a) in Fig. 3A) is located laterally behind the lateral ocellus. The nature of these fields (secretionary or sensory) could not be identified in histological sections.

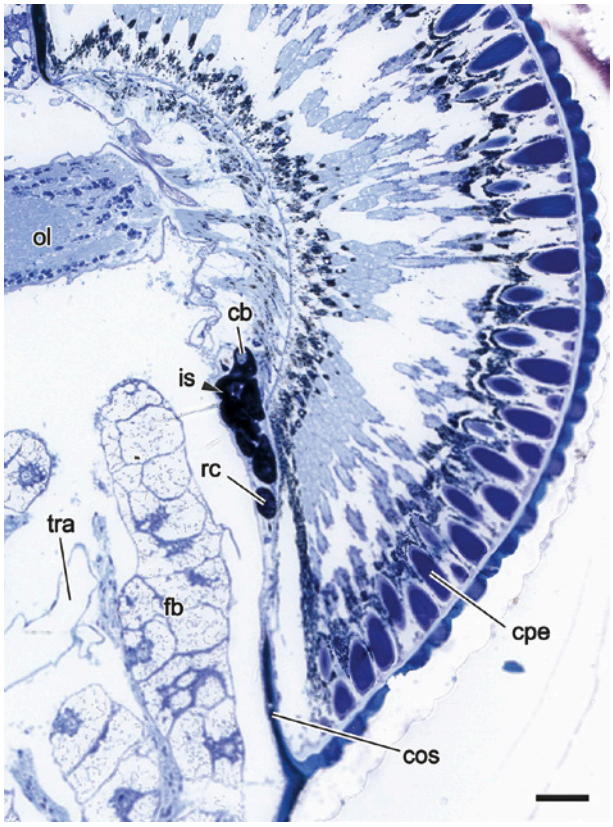

Fig. 5. *Philopotamus ludificatus* McLachlan, 1878: head, cross-section of compound eye and imaginal stemma (marked by arrow head). — ***Abbreviations***: cb – crystalline body, cos – circumocular sulcus, cpe – compound eye, fb – fat body, is – imaginal stemma, ol – optical lobe of protocerebrum, rc – retinula cell, tra – trachea. (Scale bar: 10 µm)

3.3. Tentorium

The tentorium is X-shaped with very short but stout posterior tentorial arms (pta in Fig. 14A,B) enforcing the ventrolateral margin of the alaforamen toward the condyli occipitales (Fig. 12B). The posterior tentorial pit (ptp in Fig. 12B) is located in the postoccipital sulcus. It is directed laterad (Fig. 12B). A stout tentorial bridge (tb in Fig. 14A,B) connects the posterior tentorial arms. The posterior most parts of the anterior tentorial arms are mesally fused, forming a plate-like corpotentorium (cot in Fig. 14A,B) posteriorly continuous with the tentorial bridge. The anterior tentorial arm (ata in Fig. 14A,B) is well-developed and originates in a large, rounded anterior tentorial pit which is located about half the distance between the base of the antenna and the anteclypeolabrum (atp in Figs. 1, 12A). The part of the anterior arm directly adjacent to the head capsule or the tentorial bridge is well sclerotized. Between these areas the arm becomes medio-laterally flattened with the lateral side weakly sclerotized. In this region a flattened and weakly sclerotized ventromesally directed process (laminatentorium) is developed (lt in Fig. 14A,B). The margin of the anterior tentorial pit is reinforced by the dorsally directed frontogenal sulcus (fgs in Figs. 1, 16A). A dorsal tentorial arm is weakly developed and is represented by a short peak directed dorsad (dta in Fig. 17C).

3.4. Eyes

The large, circular compound eye (cpe in Figs. 1, 5) protrudes laterally beyond the head capsule. Along its internal margin it is supported by a well-sclerotized circumocular sulcus (cos in Figs. 5, 16A) with a keyhole-shaped aperture. Each compound eye consists of app. 1,500 ommatidia. The ommatidia are covered by a dense vestiture of very fine, rounded corneal nipples (after Bernhard & Miller 1962) (ca. 130 nm in diameter) (Fig. 4B). Few interommatidial trichoid sensilla are irregularly spread on the surface of the compound eye (arrow head in Fig. 4A). Two lateral ocelli (loc in Fig. 1) are located mesally, slightly behind the midline of the compound eyes. A median ocellus (moc in Fig. 1) is located half the distance

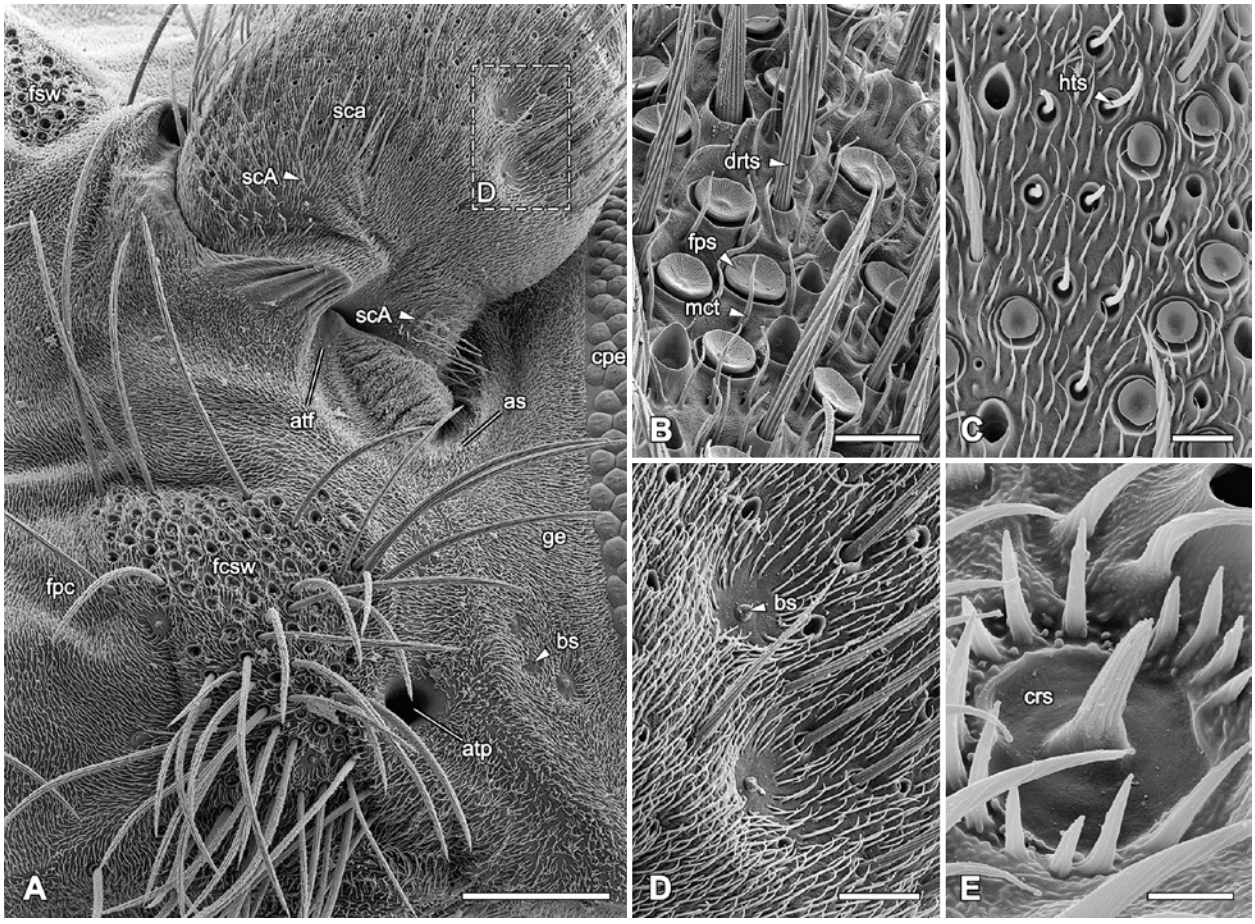

Fig. 6. *Philopotamus ludificatus* McLachlan, 1878: antenna, SEM images. **A**: anterior view on frontoclypeus and antennal base, **B**: detail of antennal sensilla and microtrichia, **C**: detail of sensory field on sixth flagellomere, **D**: detail of scapal sensilla, **E**: detail of sensillum basiconicum surrounded by a ring of microtrichia. — ***Abbreviations***: as – antennal socket, atf – antennifer, atp – anterior tentorial pit, bs – sensillum basiconicum, cpe – compound eye, crs – coronary sensillum, drts – dentate ribbed trichoid sensillum, fcsw – frontoclypeal setal wart, fpc – frontopostclypeus, fps – fungiform pseudoplacoid sensillum, fsw – frontal setal wart, ge – gena, hts – helical trichoid sensillum, mct – microtrichium, sca – scapus, scA – sensillum chaeticum A. (Scale bars: A: 100 µm; D: 20 µm; B, C: 10 µm; E: 2 µm)

between the dorsal antennal edges. An internalized imaginal stemma (is in Fig. 5) is located posteroventrally adjacent to the retinula cells of the compound eye between the optic lobe of the brain (ol in Fig. 5) and the inner edge of the circumocular sulcus (cos in Fig. 5). It is visible as a wedge-shaped assemblage of several pigment cells (rc) and at least one cone cell (cb in Fig. 5).

3.5. Antenna

The filiform antenna is almost as long as the body. It comprises on average 53 antennomeres in both sexes (49–55; n = 50). The general coloration is light brown. Scapus (sca), pedicellus (ped) and the first 24–27 flagellomeres (fl; all in Fig. 1) show a dark brown band in the proximal half (Figs. 1, 2A). The width of the band decreases along the antenna from proximal to distal. The scapus is the largest antennomere. It is almost as long as wide (sca in Figs. 1, 12A). The pedicellus (ped in Figs. 1, 12A) is the smallest antennomere (half of the size of the scapus). Flagellomeres 1 and 2 are smaller than the remaining flagellomeres. The terminal flagellomere is apically pointed.

All antennomeres except the scapus are irregularly covered by numerous dentate ribbed trichoid (drts) and fungiform pseudoplacoid sensilla (fps) (both in Fig. 6B). Additionally, each flagellomere is equipped with a few and irregularly distributed coronary sensilla (mainly in the proximal half on the dorsal side) (crs in Fig. 6E), numerous helical trichoid sensilla (distal half) (hts in Fig. 6C), and very few small basiconic sensilla (distal half). The ventrolateral side of the scapus is equipped with two basiconic sensilla (Fig. 6D). Proximally, the scapus bears two groups of sensilla chaetica A (after DRILLING & KLASS 2010; scA in Fig. 6A) which flank the articulation with the antennifer.

The antenna is attached dorsolaterally between the compound eye and the median ocellus. It is articulated with the antennifer situated at the ventral margin of the broad antennal socket (Fig. 6A). Scapus and pedicellus are similarly articulated. A ventromesal process of the scapus corresponds with a small furrow at the base of the pedicellus. The position of this articulation is shifted

by 55° in relation to the antennifer (Fig. 1). There are no specific articulations between the flagellomeres, which are separated by very short membranous areas.

Musculature (Figs. 12A, 13A, 16A,B, 17C–F): **M. tentorio-scapalis anterior** [te-sc(a)]: long, together with te-sc(l) the largest antennal muscle, O: mesal side of the anterior tentorial arm and laminatentorium, I: ventromesally at the scapal base with strong tendon (mesal of antennifer); **M. tentorio-scapalis posterior** [te-sc(p)]: slender, O: dorsally at the anterior tentorial arm (between te-sc(a)/(l)), I: dorsomesal margin of the scapal base; **M. tentorio-scapalis lateralis** [te-sc(l)]: two adjacent bundles, O: lateral face of the anterior tentorial arm and the laminatentorium (opposite to te-sc(a)), I: ventrolaterally at the scapal base (lateral of antennifer), posterior bundle with short tendon; **M. tentorio-scapalis medialis** [te-sc(m)]: comparatively short, O: dorsally on the anterior tentorial arm close to the head capsule (close to fr-ph(l)), distinctly anterior to the other antennal muscles, I: mesal margin of the scapal base; **M. scapo-pedicellaris medialis** [sc-pe(m)][2]: comprises three bundles: two lateral: O: dorsal and ventromesal areas of scapal base, I: both bundles together mesally at the pedicellar base (mesal of scapo-pedicellar articulation); one dorsal: O: between the first two bundles on the mesal face of the scapus, I: dorsally at the proximal margin of the pedicellus (almost opposite to scapo-pedicellar articulation); **M. scapo-pedicellaris lateralis** [sc-pe(l)]: two bundles, O: ventromesal and ventrolateral margin of scapal base (enclosing the scapal joint with the head capsule) I: large parts of ventral and ventrolateral margin of the pedicellus (lateral of scapo-pedicellar articulation).

3.6. Labrum

The labrum and anteclypeus together form a structural and functional unit (anteclypeolabrum, acl in Fig. 1; see above); the two components are inseparable since a clypeolabral articulation and the cranial flexor muscle (M. fronto-labralis) of the labrum are absent. The anteclypeolabrum is triangular and divided into a large, strongly sclerotized proximal part (acl(p)) and a short, membranous distal section (acl(d)) forming a rounded tip (Fig. 1).

Musculature: **M. labro-epipharyngalis** [lb-eph]: absent. **M. fronto-labralis** [fr-lb]: absent.

3.7. Mandible

The mandible (md) is largely membranous in its lateral half (md(m) in Figs. 1, 7A) which is mesally continuous with the moderately sclerotized mandibular sclerite (md(s) in Figs. 1, 7A). The short, lobe-like mandibular sclerite is antero-posteriorly flattened and lacks any teeth. The inner rims of the mandibular sclerites form blunt edges, which do not overlap but touch each other at mid-length. Proximally, the mandibular sclerites enclose the bulged mid-part of the hypopharynx (Fig. 16D). The mandibular sclerites are almost completely covered by the anteclypeolabrum and hung into distinct concavities of the latter (Fig. 16D). There are no true articulations with the head capsule. The extensive adductor tendon (adte in Fig. 16C) is largely formed by non-sclerotized cuticle and has a broad origin at the proximomesal edge of the mandible (Fig. 16C); the cuticle is not particularly thickened in this area. The abductor tendon (abte in Fig. 16D) is not connected to the mandibular sclerite but attaches to an invagination, which forms a distinct pit in the lateral mandibular membrane (Fig. 7A). This configuration does not allow notable movements of the mandible in the post-pharate stage (see also Discussion).

Musculature (Figs. 12A,B, 13A,B, 16A–D, 17D,E): **M. cranio-mandibularis medialis** [cr-md(m)]: the largest muscle of the head (fills app. ½ of the head capsule volume), composed of several bundles which aggregate toward the adductor tendon, O: large parts of the dorsal and lateral head capsule (occipital/postoccipital region, postgena and vertex posterior to postfrontal sulcus), I: adductor tendon of the mandible; **M. cranio-mandibularis lateralis** [cr-md(l)]: large but only app. ¼ of cr-md(m), O: with several bundles on the lateral area of the postgena and dorsolateral on gena and circumocular sulcus (partly between attachment areas of cr-md(m)), I: laterally at the membranous part of the mandible (close to the subgenal process) by means of the long abductor tendon; **M. hypopharyngo-mandibularis** [hy-md]: absent; **M. tentorio-mandibularis** [te-md]: extremely thin, composed of 2–3 fibers, closely adjacent with the mandibular nerve, O: anterior tentorial arm, covered by the anterior bundle of te-sc(l), I: mesally on the inner wall of the mandibular sclerite (with a long and very thin tendon).

3.8. Maxilla

The maxilla is composed of a composite basal sclerite (i.e., cardo + basistipes, dististipes), a composite galeolacinia, and a 5-segmented maxillary palp. The small cardo (cd in Figs. 2A,B, 10) forms the basalmost part of the maxilla. Distally, the cardo is completely fused with the considerably larger stipes. A strong oblique sulcus (tss in Figs. 2A,B, 10), externally visible as a dark brown stripe, separates the stipes into a proximal basistipes (bst in Figs. 2A,B, 10) which is continuous with the cardo and an apical dististipes (dst in Figs. 2A,B, 10). The lateral end of this sulcus forms a distinct dorsal apodeme serving as attachment area of the cranial muscle of the stipes, whereas the mesal end is only slightly pointed. The proximolateral angle of the cardo meets the subgena close to the adjacent postgena without forming a distinct articulation.

The proximal margin of the dististipes is almost completely fused with the composite basal piece formed by

[2] Lateral and medial reflects the relative position of the muscles to the scapo-pedicellar joint.

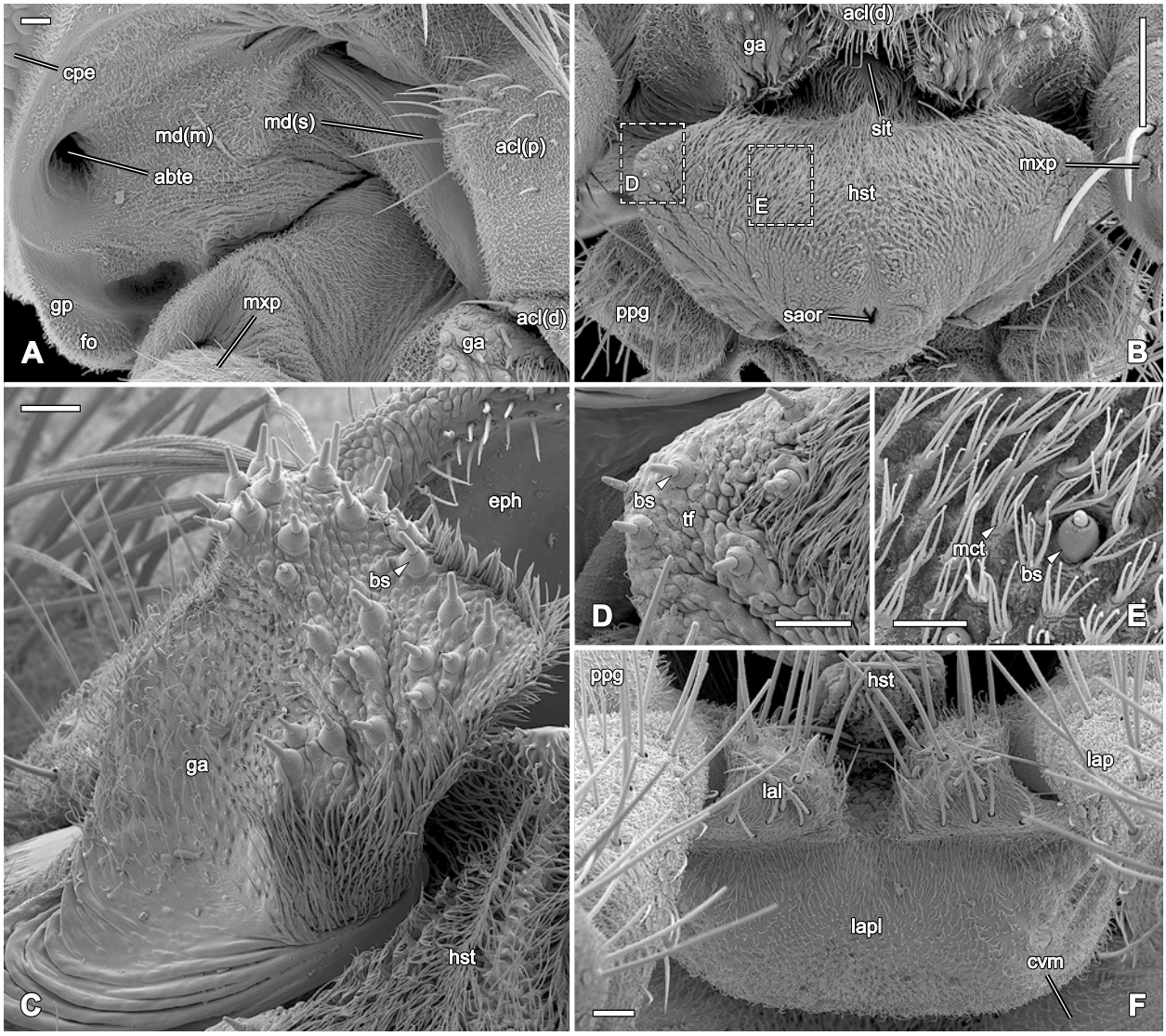

Fig. 7. *Philopotamus ludificatus* McLachlan, 1878: mouthparts, SEM images. **A**: anterior view on base of mandible, **B**: anterior view on haustellum, **C**: anterior view on galeolacinia, **D**: detail of surface of haustellum, **E**: detail of sensilla and microtrichia of haustellum, **F**: anterior view on labium. — ***Abbreviations***: abte – tendon of abductor muscle of mandible (M. cranio-mandibularis lateralis), acl(d) – distal part of anteclypeolabrum, acl(p) – proximal part of anteclypeolabrum, bs – sensillum basiconicum, cpe – compound eye, cvm – cervical membrane, eph – epipharynx, fo – fossa of subgenal process, ga – galea, gp – subgenal process, hst – haustellum, lal – labial lobe, lap – labial palp, lapl – central plate of labium, mct – microtrichium, md(m) – membranous part of mandible, md(s) – mandibular sclerite, mxp – maxillary palp, ppg – palpiger, saor – salivary orifice, sit – sitophore plate, tf – tubercular field. (Scale bars: B: 100 µm; A, C, D, F: 20 µm; E: 10 µm)

the cardo and the basistipes. It is only mesally separated by a short triangular membranous incision (tsi in Fig. 2B). The mesal margin of the trough-shaped stipes is somewhat more strongly sclerotized and forms a short distal process (msp in Fig. 10) at 2/3 of its length. The sclerite slightly widens distally bearing two terminal appendages, the large maxillary palp (mxp in Figs. 1, 2A,B) laterally and an endite lobe which presumably represents a composite structure formed by a galea and a mainly incorporated lacinia mesally (i.e., a galeolacinia, see Discussion). Most parts of the galea (ga in Figs. 8, 9A–C) are weakly sclerotized and quite flexible. Only the lateral margin is more strongly sclerotized. The lobe-like structure is dorso-ventrally flattened and apically blunted (Fig. 8). A membranous area around the base of the galea allows for substantial movements of the appendage (Fig. 7C). A small, slightly bulged lobe is located on the lower inner wall of the galea. It is separated from the latter by a small invagination of comparatively weakly sclerotized cuticle whereas its inner wall is heavily sclerotized (Fig. 9A–C). This inner lobe of the galea may represent the remnants of a lacinia (lac in Figs. 8, 9B, see Discussion), and hence this structure should be termed as a galeolacinia. The galeolacinia is located between the base of the haustellum and the maxillary palp (Fig. 7B). Its surface is densely covered by different types of sensilla. The granulose terminal face lacks microtrichia but bears several large basiconic sensilla (bs in Fig. 7C). The mesal wall is covered by a very dense vestiture of outwards directed microtrichia.

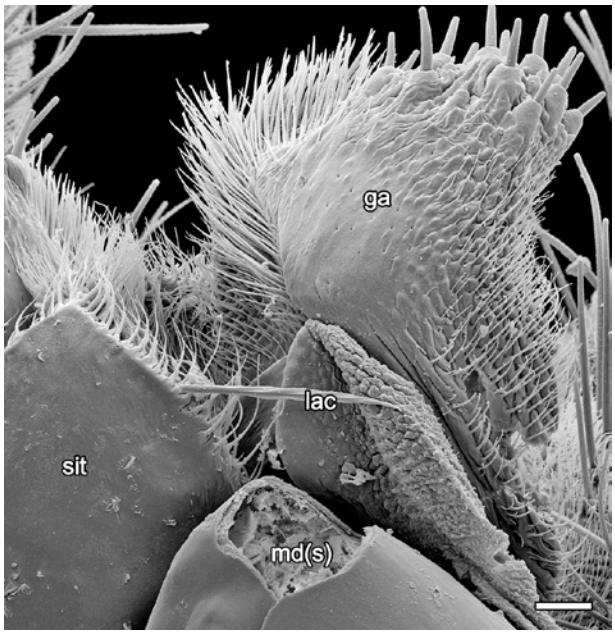

Fig. 8. *Philopotamus ludificatus* McLachlan, 1878: dorsal view on mouthparts with mandible partly removed, SEM image. — ***Abbreviations***: ga – galea, lac – lacinia, md(s) – mandibular sclerite, sit – sitophore plate. (Scale bar: 20 µm)

The large maxillary palp (mxp in Fig. 1) is 5-segmented in both sexes. It is about three times longer than the overall length of the head capsule. The 1st and 2nd palpomeres are comparatively short (together as long as the 3rd). The 3rd and the 4th palpomere are of equal length. The tapering 5th palpomere is by far the longest (almost as long as the other palpomeres together) (Fig. 1). The diameter of the palpomeres constantly decreases toward the apex. All are covered by a dense vestiture of short, dentate ribbed trichoid and fungiform pseudoplacoid sensilla (same condition as in labial palp; drts, fps in Fig. 11A,E). Additionally, the 1st and 2nd palpomeres are equipped with numerous strong, smooth ribbed trichoid sensilla (mainly on the mesal faces) (srts in Figs. 1). The 4th palpomere bears proximomesally a distinctly delimited sensory field which is composed of numerous sensilla with stout, peg-shaped trichoms (ps in Fig. 11C). The 5th palpomere is apically equipped with three basiconic sensilla. A large central sensillum basiconicum (bs) is mesally and laterally flanked by three-time shorter sensilla of this type (same ratio as in labial palp; see Fig. 11D).

Musculature (Figs. 9A,B, 10, 12A,B, 13A, 16E): **M. cranio-cardinalis** [cr-cd]: flattened, fan-shaped, O: ventrolaterally at the postgena, immediately mesally to the occipital sulcus, I: ventromesally at the proximal margin of the cardostipital sclerite (i.e., cardo + basistipes); **M. cranio-stipitalis** [cr-st]: long and slender, intersects with cr-prm(l), O: postgena, ventrally of base of the posterior tentorial arm (between cr-prm(l) and cr-prm(m)), I: distal process of mesal dististipital margin (msp) (together with te-st); **M. tentorio-cardinalis** [te-cd]: strong, slightly tapering, O: laterally at the mid part of the anterior tentorial arm, I: mesally at the distal margin of the cardostipital sclerite (i.e., cardo + basistipes); **M. tentorio-stipitalis** [te-st]: equally sized and shaped as te-cd, O: broadly at the ventral face of the laminatentorium, I: distal process of mesal dististipital margin (msp) (together with cr-st); **M. cranio-lacinialis** [cr-lc]: long and slender, O: postgena (dorsally to cr-cd), I: laterally at the small inner lobe (i.e., lacinia) of the galeolacinia; **M. stipito-lacinialis** [st-lc]: absent; **M. stipito-galealis** [st-ga]: absent; **M. cardo-palpalis dorsalis** [cd-mp(d)]: strong (app. two times stronger than st-mp(d)), O: proximomesal angle of the cardostipital sclerite, I: dorsolaterally at the base of the 1st palpomere; **M. cardo-palpalis ventralis** [cd-mp(v)]: compact, O: cardostipital sclerite, laterally of cd-mp(d), I: ventral margin of the 1st palpomere (opposite cd-mp(d)); **M. stipito-palpalis dorsalis** [st-mp(d)]: compact, O: mesally on the proximal half of the dististipes, I: mesally at the dorsal margin of the 1st palpomere (medially of cd-mp(d)); **M. palpo-palpalis maxillae primus lateralis** [mp1-mp2(l)]: two adjacent bundles, O: mesal margin of the base of palpomere 1, I: ventrolaterally at the proximal margin of palpomere 2; **M. palpo-palpalis maxillae primus medialis** [mp1-mp2(m)]: short, slightly tapering, O: mesal wall of palpomere 1 (distally of mp1-mp2(l)), I: dorsomesally at the base of palpomere 2; **M. palpo-palpalis maxillae secundus** [mp2-mp3]: compact, flattened, O: dorsal wall of palpomere 2, I: dorsolaterally at the base of palpomere 3; **M. palpo-palpalis maxillae tertius** [mp3-mp4]: slender, O: dorsally at the middle of the mesal wall of palpomere 3, I: ventromesally at the base of palpomere 4; **M. palpo-palpalis maxillae quartus** [mp4-mp5]: very thin, O: dorsomesally on the distal half of palpomere 4, I: ventromesally at the base of palpomere 5.

3.9. Labium

The main body of the labium is bulged, pillow-shaped and weakly sclerotized (Figs. 2B, 7F). Posteriorly, it is continuous with the cervical membrane (cvm in Fig. 2B). A non-pigmented central labial plate (lapl in Figs. 2B) is delimited from the cervix by a semicircular fold (laf in Fig. 2B). This fold might represent the posterior margin of the labium, but the homology of the central plate is uncertain (see Discussion). The degree of sclerotization increases from the proximal to the distal parts (Fig. 2B). There are no traces of subdivision. Laterally, it is not distinctly delimited from the surrounding membrane. The distal face of the labial plate bears a small lobe (lal in Fig. 7F) mesally to the base of the labial palp (lap in Figs. 7F, 10). This lobe is covered with several stout smooth ribbed trichoid sensilla and is not equipped with intrinsic muscles. Laterally, the prementum forms a moderately sclerotized palpiger (ppg in Fig. 7B). This sclerite surrounds the base of the labial palp forming the anterolateral edge of the labium. The surface of the palpiger is equipped with stout smooth ribbed trichoid sensilla. The labial palp is 3-segmented in both sexes and located distally on the premental palpiger. Both elements

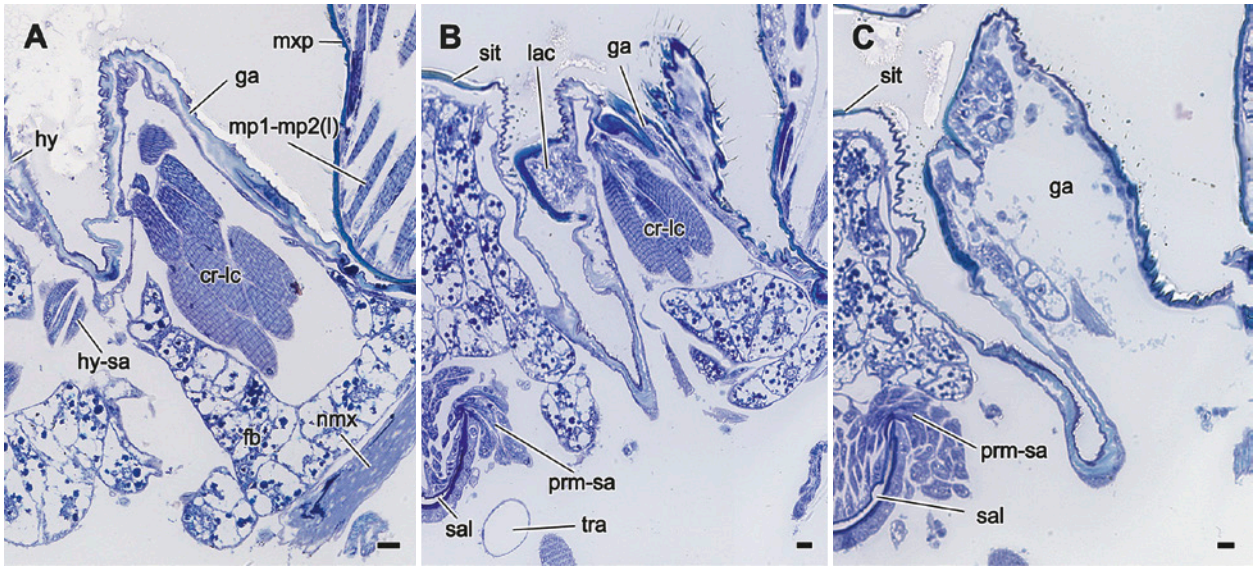

Fig. 9. *Philopotamus ludificatus* McLachlan, 1878: head, histological section of galeolacinia. **A**: proximal part of galea, **B**: galea with incorporated lacinia, **C**: distal part of galea. — ***Abbreviations***: cr-lc – M. cranio-lacinialis, fb – fat body, ga – galea, lac – lacinia, hy – hypopharynx, hy-sa – M. hypopharyngo-salivarialis, mp1-mp2(l) – M. palpo-palpalis maxillae primus lateralis, mxp – maxillary palp, nmx – maxillary nerve, prm-sa – M. praemento-salivarialis, sal – salivarium, sit – sitophore plate, tra – trachea. (Scale bars: 10 µm)

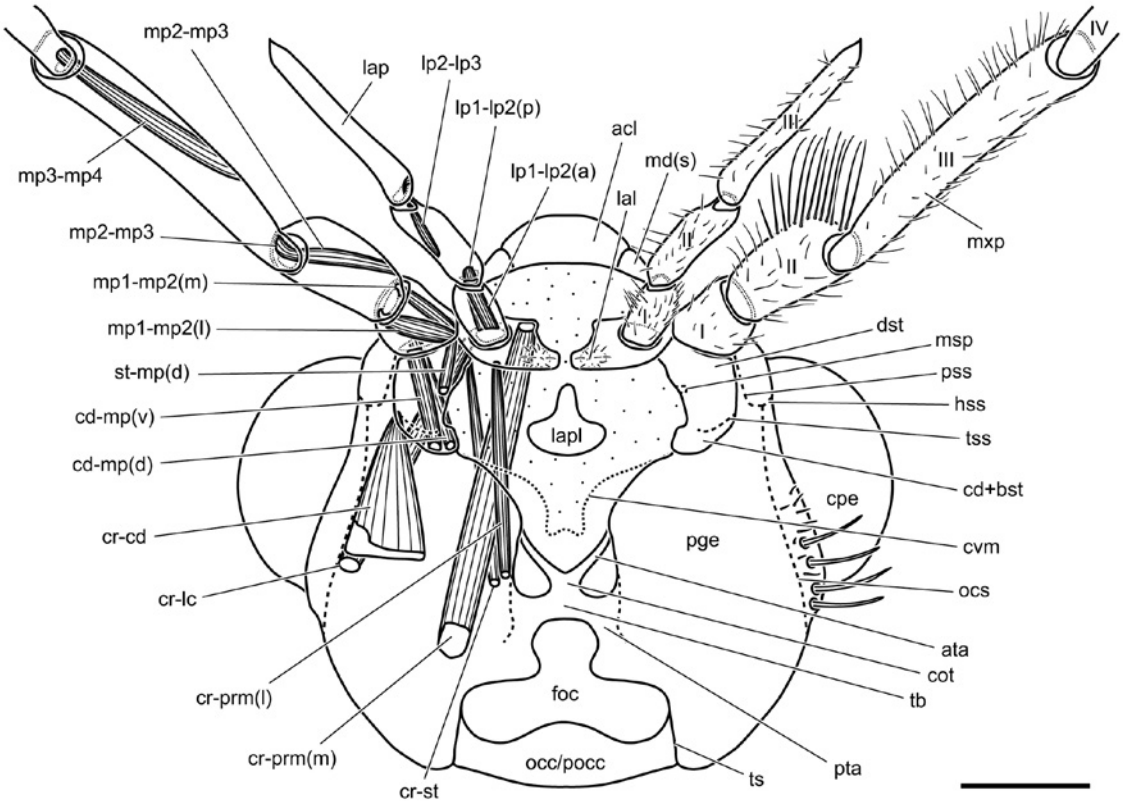

Fig. 10. *Philopotamus ludificatus* McLachlan, 1878: head, posterior view. — ***Abbreviations***: acl – anteclypeolabrum, ata – anterior tentorial arm, bst – basistipes, cd – cardo, cd-mp(d) – M. cardo-palpalis dorsalis, cd-mp(v) – M. cardo-palpalis ventralis, cot – corpotentorium, cpe – compound eye, cr-cd – M. cranio-cardinalis, cr-lc – M. cranio-lacinialis, cr-prm(l) – M. cranio-praementalis lateralis, cr-prm(m) – M. cranio-praementalis medialis, cr-st – M. cranio-stipitalis, cvm – cervical membrane, dst – dististipes, foc – foramen occipitale, hss – hypostomal sulcus, lal – labial lobe, lap – labial palp, lapl – labial plate, lp1-lp2(a) – M. palpo-palpalis labii primus anterior, lp1-lp2(p) – M. palpo-palpalis labii primus posterior, lp2-lp3 – M. palpo-palpalis labii secundus, md(s) – mandibular sclerite, mp1-mp2(l) – M. palpo-palpalis maxillae primus lateralis, mp1-mp2(m) – M. palpo-palpalis maxillae primus medialis, mp2-mp3 – M. palpo-palpalis maxillae secundus, mp3-mp4 – M. palpo-palpalis maxillae tertius, mxp – maxillary palp, msp – mesal process of dististipes, occ – occiput, ocs – occipital sulcus, pge – postgena, pocc – postocciput, pss – pleurostomal sulcus, pta – posterior tentorial arm, st-mp(d) – M. stipito-palpalis dorsalis, tb – tentorial bridge, ts – temporal sulcus, tss – transstipital sulcus, I–IV – number of palpomere. (Scale bar: 250 µm)

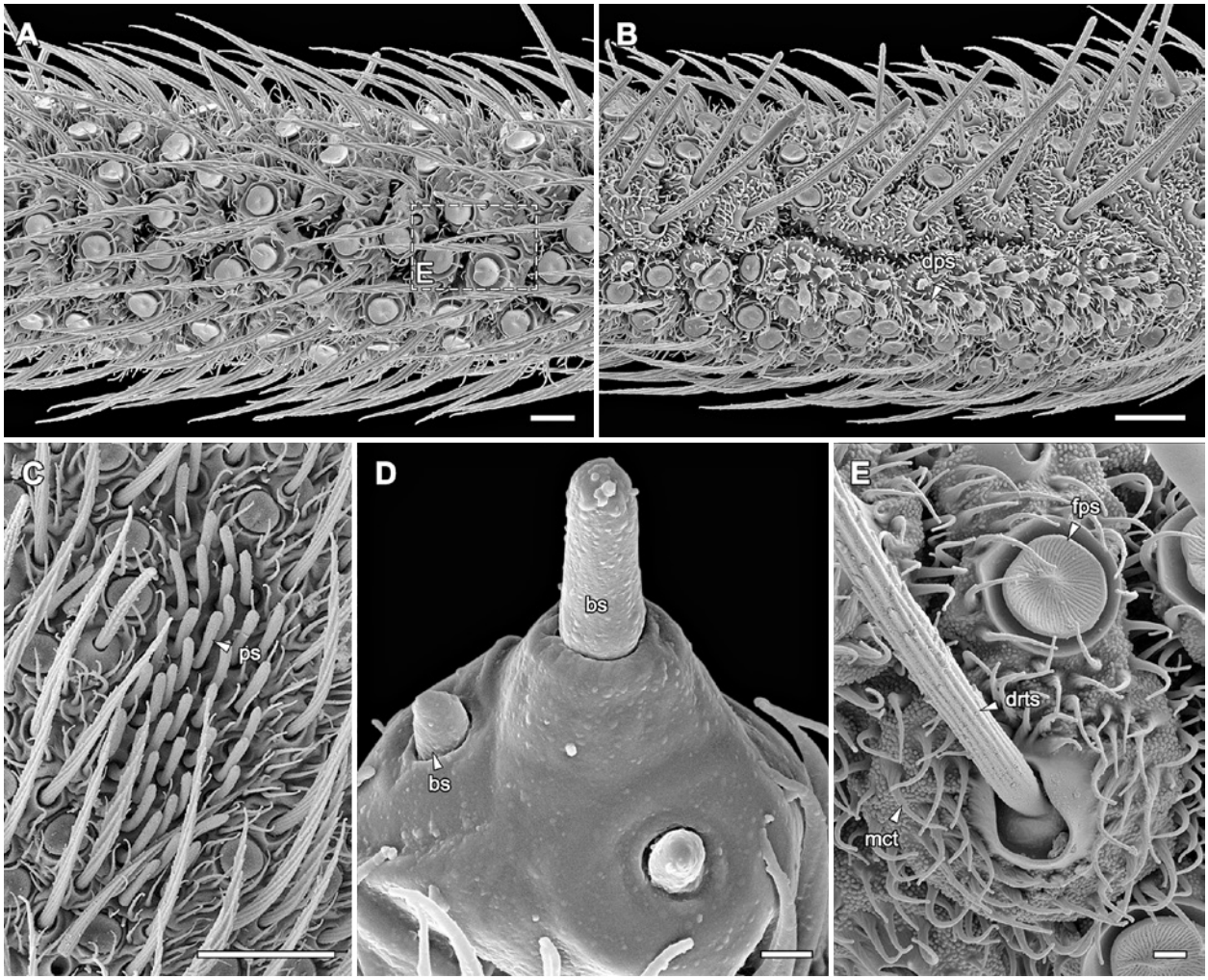

Fig. 11. *Philopotamus ludificatus* McLachlan, 1878: mouthparts, SEM images. **A**: lateral wall of third palpomere of labial palp, **B**: mesal wall of third palpomere of labial palp with sensory field of dentate pseudoplacoid sensilla, **C**: lateral wall of maxillary palp with sensory field of peg-like sensilla, **D**: tip of labial palp with basiconic sensilla, **E**: detail of sensilla and microtrichia of labial palp. — ***Abbreviations***: bs – sensillum basiconicum, dps – dentate pseudoplacoid sensillum, drts – dentate ribbed trichoid sensillum, fps – fungiform pseudoplacoid sensillum, mct – microtrichium, ps – peg-like sensillum. (Scale bars: B, C: 20 µm; A: 10 µm; E: 2 µm; D: 1 µm)

are distinctly separated by an extensive articulary membrane; no specific skeletal articulation is developed. The 2nd palpomere is almost as long as the 1st. The tapering 3rd palpomere is as long as segments 1 and 2 together (Fig. 1). All labial palpomeres are covered by a dense vestiture of short dentate ribbed trichoid and fungiform pseudoplacoid sensilla (drts, fps in Fig. 11A,E). A discrete, elongate sensory field composed of app. 30 dentate pseudoplacoid sensilla is located mesally in the proximal half of the 3rd palpomere (Fig. 11B). The tip of the 3rd palpomere bears four basiconic sensilla: a large central sensillum is surrounded by three smaller ones (Fig. 11D).

Musculature (Figs. 10, 12A,B, 13A,B, 16D–F): **M. cranio-praementalis medialis** [cr-prm(m)]: strong, composed of two more or less distinct bundles, O: both bundles closely adjacent mesally at the postgena (laterally of posterior tentorial pits, dorsolaterally of cr-st), I: broadly at the distal part of the prementum, bundles more or less distinctly separated mesally and laterally of prm-lp(m); **M. cranio-praementalis lateralis** [cr-prm(l)]: long, slender (app. ⅔ thinner as cr-prm(m)), O: postgena, ventrally of posterior tentorial pit and directly mesally of cr-st, I: lateral rim of palpiger; **M. submento-praementalis** [smt-prm]: absent; **M. praemento-paraglossalis** [prm-pgl]: absent; **M. praemento-glossalis** [prm-gl]: absent; **M. praemento-palpalis medialis** [prm-lp(m)]: slender, comparatively long, O: mesally at the dorsal face of the prementum (close to the base of haustellum, between bundles of cr-prm(m)), I: laterally at the proximal margin of palpomere 1; **M. praemento-palpalis lateralis** [prm-lp(l)]: compact, O: proximolaterally on palpiger, I: laterally at the proximal margin of palpomere 1 (close to prm-lp(m)); **M. palpo-palpalis labii primus anterior** [lp1-lp2(a)]: O: anterolaterally at the base of palpomere 1, I: anteriorly at the base of palpomere 2; **M. palpo-palpalis labii primus posterior** [lp1-lp2(p)]: O: posteriorly at the base of palpomere 1, I: posteriorly at the base of palpomere 2; **M. palpo-palpalis labii secundus** [lp2-lp3]: thin, O: anterolaterally at the distal half of palpomere 2, I: laterally at the proximal margin of palpomere 3.

3.10. Epipharynx and hypopharynx

The epipharynx (eph in Figs. 7C, 16D), that is, the inner wall of the anteclypeolabrum, is strongly sclerotized and positioned between the mandibles in its ventral half, forming the roof of the preoral cavity (= cibarium) (poc in Fig. 13B). The narrow, somewhat bulged epipharynx is only continuous with the sclerotized lateral margin of the anteclypeolabrum at its distal end. It is laterally surrounded by membranous regions in the other parts. The epipharyngeal sclerite terminates dorsally at the beginning of the closed prepharyngeal tube (see below).

The hypopharynx is composed of a mainly membranous, ventral section (i.e., anterior surface of the haustellum between the functional mouth opening and the salivary orifice) and the dorsal sitophore plate (sensu CHAUDONNERET 1990). The ventral part of the sitophore (sit in Figs. 8, 16C) is broadly underlying the distal half of the mandibles (Fig. 16D). It narrows dorsally and bulges between the mandibular bases. Before the beginning of the prepharyngeal tube (i.e., the lateral union of hypo- and epipharynx) (ppt in Figs. 13B, 16C) the sitophore plate is deeply transversely folded and continues toward the anatomical mouth opening (below the frontal ganglion) (Fig. 17F). This part of the sitophore plate forms the sclerotized floor of the prepharynx terminating in a spoon-shaped median process (sps in Fig. 13B), which projects into the prepharyngeal lumen (Figs. 13B, 17F). The sitophore lacks any sensilla (i.e., chemoreceptors) along its entire surface. The membranous roof of the prepharyngeal tube is formed by the epipharynx. The prepharynx is encircled by a thick layer of ring muscle fibers (Fig. 16C).

Musculature (Figs. 12A,B, 13A,B, 16A–C, 17C,D, F,G): **M. clypeo-epipharyngalis medialis** [cl-eph(m)]: compact, fan-shaped, O: central at the beginning of the sclerotized part of the anteclypeolabrum, I: median at the distal end of the epipharynx; **M. clypeo-epipharyngalis lateralis** [cl-eph(l)]: strong, compact, O: laterally at proximal half of the anteclypeolabrum (between cl-eph(m) and horizontal furrow), I: mesally at the epipharynx dorsad cl-eph(m); **M. clypeo-cibarialis ventralis** [cl-ci(v)]: slender, O: dorsolaterally at the anteclypeolabrum (dorsally of cl-eph(l)), I: preoral cavity at the ventralmost part of the prepharyngeal tube (dorsally of epipharyngeal sclerite), between prepharyngeal ring muscle fibers; **M. clypeo-cibarialis dorsalis** [cl-ci(d)]: two distinct bundles, compact median bundle app. two times larger than the slender lateral bundle, O: mesally (median bundle) and laterally (lateral bundle) at the frontopostclypeus, dorsally to the horizontal furrow, I: lateral bundle: proximal edge of the membranous (epipharyngeal) part of the prepharyngeal tube, directly below the ganglion frontale, median bundle: ventromesally of lateral bundle; **M. tentorio-sitophorialis** [te-si]: slender, O: paramedian on the ventral side of the tentorial bridge (between the anterior tentorial arms), I: dorsal end of the sitophore plate (below the spoon-shaped process), opposite to cl-ci(v); **M. anularis cibarialis** [an-ci]: series of ring muscle fibers covering the prepharynx, dorsally not delimited from the pharyngeal ring musculature (an-ph).

3.11. Haustellum

The distal region of the hypopharynx is fused with the labium, forming an extensive, largely membranous and eversible lobe, the haustellum (hst in Figs. 1, 7B,C). The haustellum is located between the galeolaciniae (dorsolateral), the bases of the maxillary and labial palps (ventrolateral) and the labial lobes (posterior) (Figs. 7B, 16F). It is dorsally continuous with the sitophore (see above) and below it forms a keel between the galeolaciniae (Fig. 7C). Behind the galeolaciniae the haustellum extends

→ **Fig. 12.** *Philopotamus ludificatus* McLachlan, 1878: head, 3D-reconstruction based on µCT data. **A**: anterior view, **B**: posterior view. — ***Colors***: blue – skeleton (sclerotized), light blue – eyes, green – gut, orange – musculature, rose – glands, yellow – nervous system. — ***Abbreviations***: acl(d) – distal part of anteclypeolabrum, acl(p) – proximal part of anteclypeolabrum, ata – anterior tentorial arm, atf – antennifer, atp – anterior tentorial pit, br – brain, cco – cervical connective, cd-mp(d) – M. cardo-palpalis dorsalis, cd-mp(v) – M. cardo-palpalis ventralis, cl-ci(d) – M. clypeo-cibarialis dorsalis, cl-ci(v) – M. clypeo-cibarialis ventralis, cl-eph(l) – M. clypeo-epipharyngalis lateralis, cl-eph(m) – M. clypeo-epipharyngalis medialis, cocc – condyli occipitales, cpe – compound eye, cr-cd – M. cranio-cardinalis, cr-lc – M. cranio-lacinialis, cr-md(l) – M. cranio-mandibularis lateralis, cr-md(m) – M. cranio-mandibularis medialis, cr-ph(a) – M. cranio-pharyngalis anterior, cr-prm(l) – M. cranio-praementalis lateralis, cr-prm(m) – M. cranio-praementalis medialis, cr-st – M. cranio-stipitalis, cvm – cervical membrane, foc – foramen occipitale, fg – ganglion frontale, fr-ph(a) – M. fronto-pharyngalis anterior, fr-ph(p) – M. fronto-pharyngalis posterior, ga – galea, gp – subgenal process, hf – horizontal furrow between frontopostclypeus and anteclypeolabrum, hst – haustellum, lap – labial palp, loc – lateral ocellus, lp1-lp2 – M. palpo-palpalis labii primus [lp1-lp2(a) and lp1-lp2(p) together], md(s) – mandibular sclerite, moc – median ocellus, mp1-mp2(l) – M. palpo-palpalis maxillae primus lateralis, mp1-mp2(m) – M. palpo-palpalis maxillae primus medialis, mp2-mp3 – M. palpo-palpalis maxillae secundus, occ – occiput, oes – oesophagus, ped – pedicellus, pocc – postocciput, prm-lp(l) – M. praemento-palpalis lateralis, prm-lp(m) – M. praemento-palpalis medialis, prm-sa – M. praemento-salivarialis, pta – posterior tentorial arm, ptp – posterior tentorial pit, sc-pe(l) – M. scapo-pedicellaris lateralis, sc-pe(m) – M. scapo-pedicellaris medialis, sca – scapus, sd – salivary duct, soeg – suboesophageal ganglion, st-mp(d) – M. stipito-palpalis dorsalis, tb – tentorial bridge, te-cd – M. tentorio-cardinalis, te-md – M. tentorio-mandibularis, te-ph(a) – M. tentorio-pharyngalis anterior, te-ph(l) – M. tentorio-pharyngalis lateralis, te-ph(p) – M. tentorio-pharyngalis posterior, te-sc(a) – M. tentorio-scapalis anterior, te-sc(l) – M. tentorio-scapalis lateralis, te-sc(m) – M. tentorio-scapalis medialis, te-sc(p) – M. tentorio-scapalis posterior, te-si – M. tentorio-sitophorialis, te-st – M. tentorio-stipitalis, tra – trachea, vsw(p) – posterior setal wart of vertex. (Scale bars: 250 µm) (General features of nervous system shown, for details see Fig. 18)

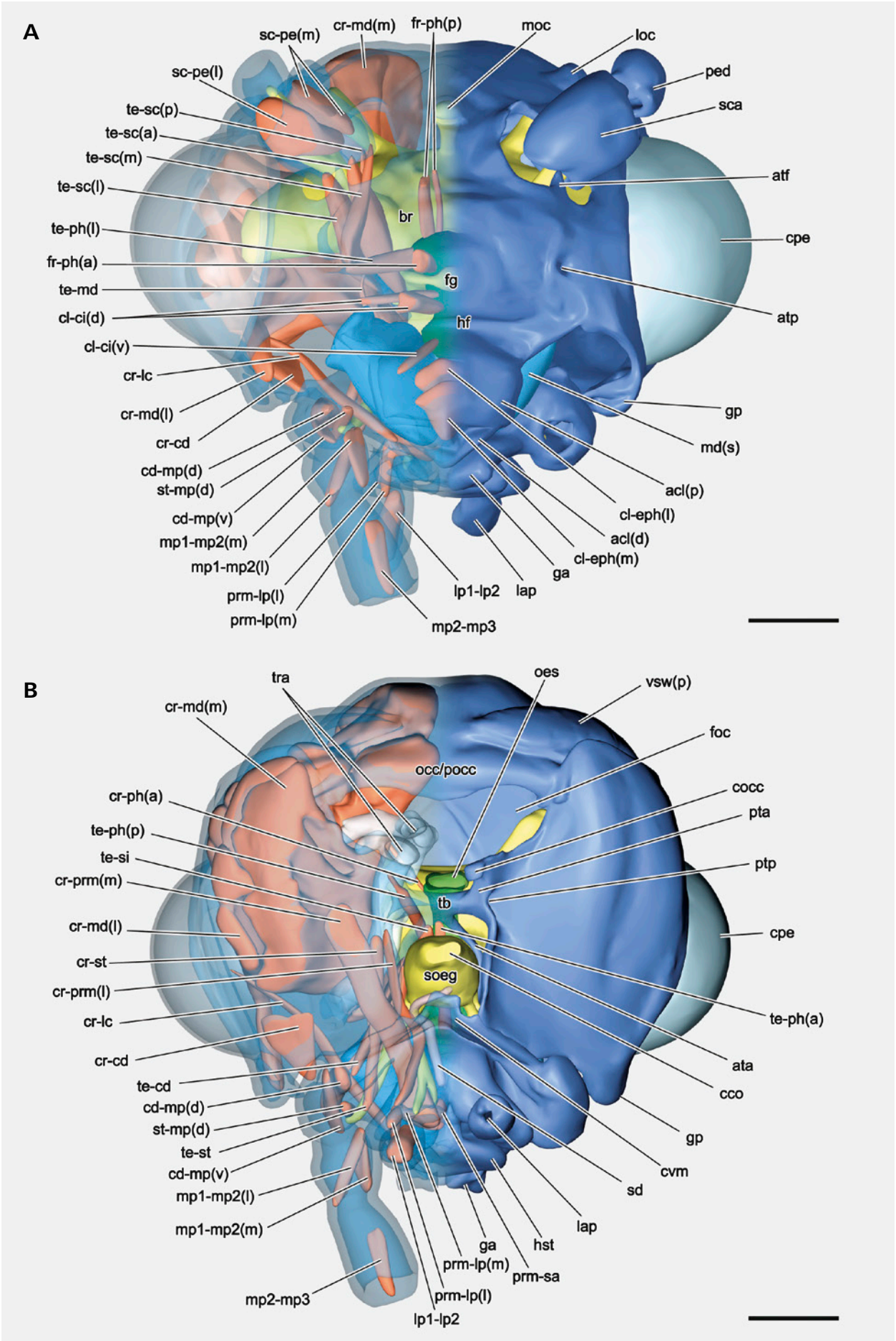
A
sc-pe(m)
cr-md(m)
fr-ph(p)
moc
loc
ped
sca
atf
cpe
atp
gp
md(s)
acl(p)
cl-eph(l)
acl(d)
cl-eph(m)
ga
lap
lp1-lp2
mp2-mp3
prm-lp(m)
prm-lp(l)
mp1-mp2(l)
mp1-mp2(m)
cd-mp(v)
st-mp(d)
cd-mp(d)
cr-cd
cr-md(l)
cr-lc
cl-ci(v)
cl-ci(d)
te-md
fr-ph(a)
te-ph(l)
te-sc(l)
te-sc(m)
te-sc(a)
te-sc(p)
sc-pe(l)
br
fg
hf
B
tra
oes
vsw(p)
foc
cocc
pta
ptp
cpe
te-ph(a)
ata
cco
gp
cvm
sd
lap
hst
prm-sa
ga
prm-lp(m)
prm-lp(l)
lp1-lp2
mp2-mp3
mp1-mp2(m)
mp1-mp2(l)
cd-mp(v)
te-st
st-mp(d)
cd-mp(d)
te-cd
cr-cd
cr-lc
cr-prm(l)
cr-st
cr-md(l)
cr-prm(m)
te-si
te-ph(p)
cr-ph(a)
cr-md(m)
occ/pocc
tb
soeg

laterally till the bases of the maxillary and labial palps. This anterior, upper area is densely covered by multibranched, irregularly distributed microtrichia (mct in Fig. 7E) more or less directed toward the preoral cavity. A regular system of channels on the surface of the haustellum is not present (Fig. 7B–E). The posterior part of the haustellum converges toward the labial lobes (Fig. 7F). Its lower surface is glabrous and tubercular (Fig. 7D). Centrally, on this anterior area terminates the salivarium (see below). A median crest with a moderately dense set of microtrichia connects the salivary orifice and the preoral cavity (Fig. 7C). Basiconic sensilla (bs in Fig. 7E) of different sizes are randomly distributed on the whole face of the haustellum.

3.12. Salivarium

The long, tubular salivary glands (sg in Fig. 17H) extend into the cervical and prothoracic regions. Anteriorly two thin salivary ducts (sd in Fig. 17H) enter the head capsule through the lower section of the occipital foramen (below the suboesophageal ganglion) and unite at the beginning of the unpaired salivarium (sal in Figs. 13B, 17I). The sclerotized salivarium is U-shaped in cross section and rapidly increases its caliber in the proximal half (Fig. 16E,F). The distal part (after the muscle insertion areas) is tapering toward the orifice. Its strongly concave floor (fsal in Fig. 16E,F) is heavily sclerotized. The less sclerotized pestle-like roof (rsal in Fig. 16E,F) sinks into the concavity of the floor. The salivary orifice is located on the lower, anterior edge of the haustellum (saor in Fig. 7B). The opening is surrounded by numerous small, two- to three-branched microtrichia.

Musculature (Figs. 13B, 16E,F, 17I): **M. hypopharyngo-salivarialis** [hy-sa]: compact, slender, O: laterally at the ventral half of the sitophore, close to the base of the galeolacinia, I: proximally on the roof of the salivarium; **M. praemento-salivarialis** [prm-sa]: ventral part of the prementum (close to prm-lp(m) and the mesal bundle of cr-prm(m)), I: proximal half of the roof of the salivarium (immediately laterally and before hy-sa); **M. intra-salivarialis** [i-sa]: absent.

3.13. Cephalic food tract

The cephalic food tract comprises a distinctly widened precerebral pumping chamber (pch in Fig. 18A) (= buccal cavity, i.e. a composite formation of the prepharyngeal tube [ppt] and the precerebral pharynx [pph in Fig. 13B]). The border between both elements, i.e. the anatomical mouth opening, is marked by the position of the ganglion frontale (fg in Figs. 13B, 18A). The precerebral pumping chamber is moved by strong cibarial and pharyngeal dilator muscles. Posteriorly, the pharynx (ph in Fig. 13B) tapers distinctly before passing the tritocerebral commissures (trc in Fig. 18B). The straight intra-/postcerebral pharyngeal regions have a constant, comparatively small width (⅓ of diameter of the precerebral pharynx) (Fig. 13B).

Musculature of the precerebral pharynx (Figs. 12A, 13A,B, 16A–C, 17B,C, 18A): **M. fronto-pharyngalis anterior** [fr-ph(a)]: compact, O: central region of frontopostclypeus, between the anterior tentorial pits, I: mesally at the anterolateral corner of the precerebral pumping chamber, directly behind the ganglion frontale; **M. fronto-pharyngalis posterior** [fr-ph(p)]: two distinct bundles, ventral bundle app. two times larger than dorsal bundle, both bundles are closely associated with the precerebral part of the cephalic aorta, O: frons, mesally of interantennal sulcus, I: dorsally at the posterodorsal face of the pharyngeal pumping chamber, just in front of the brain; **M. tentorio-pharyngalis lateralis** [te-ph(l)]: strong, O: broad area of the distal half of the anterior tentorial arm, I: dorsolaterally at the pharyngeal pumping chamber; **M. tentorio-pharyngalis anterior** [te-ph(a)]: two long and slender bundles, O: mesally on the base of the anterior tentorial arm, I: ventrally at the posterior end of the pharyngeal pumping chamber (opposite to fr-ph(p)).

Musculature of the postcerebral pharynx (Figs. 13B, 16A–C, 18A): **M. tentorio-pharyngalis posterior** [te-ph(p)]: slender, O: posterior tentorial arm, I: ventrally at the postcerebral pharynx, slightly behind the brain, opposite to cr-ph(a); **M. cranio-pharyngalis anterior** [cr-ph(a)]: very thin, composed of very few fibers, O: vertex, mesally of postgenal sulcus (posteriorly of lateral ocellus), I: dorsally on postcerebral pharynx, directly behind the brain; **M. cranio-pharyngalis posterior** [cr-ph(p)]: absent.

Musculature of the entire pharynx (pre- and postcerebral regions) (Figs. 16B,C, 17C,F): **M. anularis pharyngalis** [an-ph]: series of ring muscles covering the surface of the entire pharynx, most heavily developed around the precerebral pharyngeal pumping chamber; forming a distinctly thinner layer along the postcerebral pharynx. **M. longitudinalis pharyngalis** [lo-ph]: series of longitudinal muscle fibers stretching between the surface of the pharynx and an-ph, the layer is of constant thickness in the pre- and postcerebral regions.

3.14. Central nervous system (CNS)

The brain is located in the dorsal half of the head capsule between the large compound eyes. The large protocerebrum forms laterally the optical lobes (ol in Fig. 16A), which are of similar diameter as the rest of the brain (Fig. 18A,B). One compact anteromedian nerve and two posterolateral nerves arising from the dorsal protocerebral surface supply the median ocellus and the lateral ocelli, respectively (Fig. 18A).

The deutocerebral olfactory lobe (dol in Fig. 16A) is located paramedially on the anterodorsal edge of the brain. It is not externally delimited from the deutocerebrum (Figs. 17B, 18A). The strong antennal nerve (nan in Fig. 18A,B) proximally innervates the tentorio-scapal

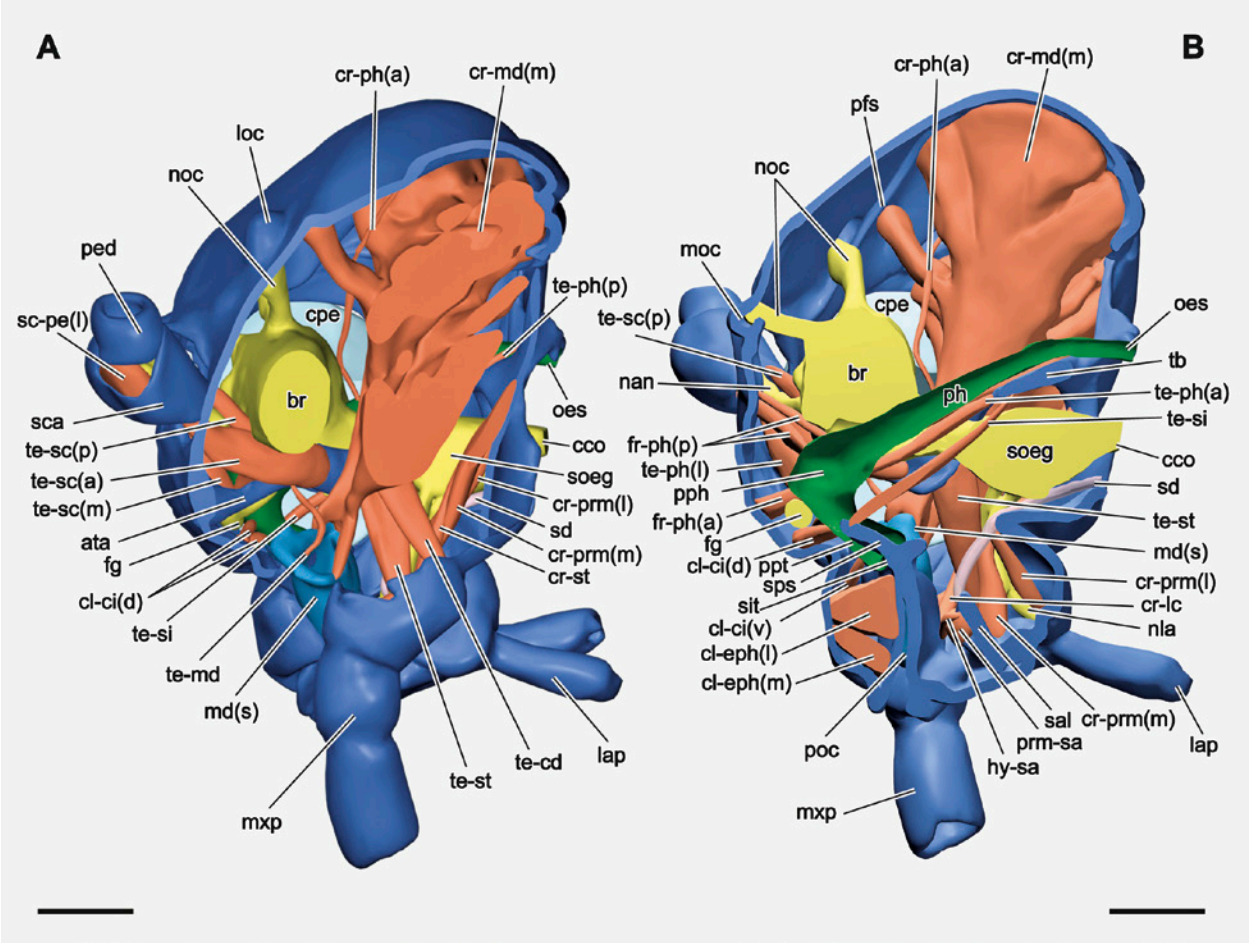

Fig. 13. *Philopotamus ludificatus* McLachlan, 1878: head, 3D-reconstruction based on µCT data. **A**: parasagittal section (level of anterior tentorial pit), **B**: sagittal section. — ***Colors***: blue – skeleton (sclerotized), light blue – eyes, green – gut, orange – musculature, rose – glands, yellow – nervous system. — ***Abbreviations***: ata – anterior tentorial arm, br – brain, cco – cervical connective, cl-ci(d) – M. clypeo-cibarialis dorsalis, cl-ci(v) – M. clypeo-cibarialis ventralis, cl-eph(l) – M. clypeo-epipharyngalis lateralis, cl-eph(m) – M. clypeo-epipharyngalis medialis, cpe – compound eye, cr-lc – M. cranio-lacinialis, cr-md(m) – M. cranio-mandibularis medialis, cr-ph(a) – M. cranio-pharyngalis anterior, cr-prm(l) – M. cranio-praementalis lateralis, cr-prm(m) – M. cranio-praementalis medialis, cr-st – M. cranio-stipitalis, fg – ganglion frontale, fr-ph(a) – M. fronto-pharyngalis anterior, fr-ph(p) – M. fronto-pharyngalis posterior, hy-sa – M. hypopharyngo-salivarialis, lap – labial palp, loc – lateral ocellus, md(s) – mandibular sclerite, moc – median ocellus, mxp – maxillary palp, nan – nervus antennalis, nla – labial nerve, noc – ocellar nerve, oes – oesophagus, ped – pedicellus, pfs – postfrontal sulcus, ph – pharynx, poc – preoral cavity, pph – precerebral pharynx, ppt – prepharyngeal tube, prm-sa – M. praemento-salivarialis, sal – salivarium, sca – scapus, sc-pe(l) – M. scapo-pedicellaris lateralis, sd – salivary duct, sit – sitophore plate, soeg – suboesophageal ganglion, sps – spoon-shaped process of sitophore plate, tb – tentorial bridge, te-cd – M. tentorio-cardinalis, te-md – M. tentorio-mandibularis, te-ph(a) – M. tentorio-pharyngalis anterior, te-ph(l) – M. tentorio-pharyngalis lateralis, te-ph(p) – M. tentorio-pharyngalis posterior, te-sc(a) – M. tentorio-scapalis anterior, te-sc(m) – M. tentorio-scapalis medialis, te-sc(p) – M. tentorio-scapalis posterior, te-si – M. tentorio-sitophorialis, te-st – M. tentorio-stipitalis. (Scale bars: 250 µm) (General features of nervous system shown, for details see Fig. 18)

muscles with thin nerve fibers before entering the scapus. It splits into two equally strong branches at the base of the antenna.

The ventral portion of the brain is formed by the tritocerebrum, which is also not externally delimited from the other parts. The tritocerebrum forms anterior lobes and the circumoesophageal connectives (coc in Fig. 18B) of the CNS. They are interconnected by a short free tritocerebral commissure (trc in Fig. 18B) below the pharynx, extending between the tentorial muscles of the sitophore plate and the ventral pharynx (te-si, te-ph(a)) (Figs. 17F, 18B). A thin nervus tegumentalis emerges from the posterolateral face of the dorsal part of the tritocerebrum. It runs dorsolaterad into the large posterolateral setal wart of the vertex.

The somewhat egg-shaped suboesophageal ganglion (soeg in Figs. 13B, 18B) is located below the postpharynx, between the posterior margin of the brain and the neuroforamen. Its posterior end is continuous with the paired cervical connectives (cco in Fig. 18B). The comparatively thin mandibular nerve arises at its anterior edge. The mandibular nerve (nmd in Fig. 18A,B) passes the mesal side of the anterior tentorial arm (at level of the laminatentorium) and splits into several bundles associat-

Table 1. Terminology and homology of the trichopteran adult head musculature. Muscles are named by their areas of origin and insertion. The musculature described for *Philopotamus* (Annulipalpia) is homologized with muscles described for 'Spicipalpia' (KLEMM 1966: *Rhyacophila*), Integripalpia (CRICHTON 1957: *Phryganea*) and basal lepidopterans (HANNEMANN 1956: *Micropterix*). General nomenclatures of the insect head muscles (v. KÉLER 1955; WIPFLER et al. 2011) are also assigned. Squared brackets indicate that the muscle description was extracted from the literature, because it is absent in *Philopotamus*. Abbreviations used: **X** = present, **–** = absent, **?** = uncertain homology, ***** = revised information taken from KRISTENSEN 2003, **n.a.** = no information available.

Name	**Abbrev.**	**Origin**	**Insertion**	**v. Kéler 1955**	**Wipfler et al. 2011**	**Hannemann 1956**	**Klemm 1966**	**Crichton 1957**	**present study**
						Micropterix	*Rhyacophila*	*Phryganea*	*Philopotamus*
M. fronto-labralis	fr-lb	[mesally on frons]	[mesally on outer basal wall of labrum]	8	0lb1	19	–	–	–
M. fronto-epipharyngalis	fr-eph	[mesally on frons]	[basal labral wall]	9	0lb2	–	mlrp (?)	–	–
M. labro-epipharyngalis	lb-eph	[outer wall of labrum]	[epipharynx]	7	0lb5	21	–	–	–
M. clypeo-epipharyngalis medialis	cl-eph(m)	distomedian at anteclypeolabrum	distal at epipharynx	43, 7 (?)	0ci1, 0lb5 (?)	20	1cplr	1	X
M. clypeo-epipharyngalis lateralis	cl-eph(l)	lateral at anteclypeolabrum	epipharynx	43	0ci1	45	2cplr	2	X
M. clypeo-cibarialis ventralis	cl-ci(v)	proximal at anteclypeolabrum	anteroventral at cibarium	44 (?)	0bu1 (?)	–	2dlcb, 1dlcb (?)	21, 22 (?)	X
M. clypeo-cibarialis dorsalis	cl-ci(d)	frontoclypeus, directly below frontal ganglion	anteroventral at cibarium	44	0bu1	49 (?)	1dlphy, 1dlcb (?)	21, 22	X (2 bundles)
M. tentorio-sitophorialis	te-si	tentorial bridge	dorsal margin of sitophore	48	0bu5	46	pdlcb	23	X
M. fronto-pharyngalis anterior	fr-ph(a)	frontoclypeus, directly behind frontal ganglion	dorsal at precerebral pharynx (anterior)	45	0bu2	48 (?)	4dlphy	24	X
M. fronto-pharyngalis posterior	fr-ph(p)	frontoclypeus	dorsal at precerbral pharynx (posterior), in front of supra-oesophageal ganglion	46	0bu3	50	2dlphy	25	X (2 bundles)
M. tentorio-pharyngalis lateralis	te-ph(l)	distal at anterior tentorial arm	lateral at precerbral pharynx	47 (?)	0hy2 (?)	48 (?)	3dlphy	26 (?)	X
M. tentorio-pharyngalis anterior	te-ph(a)	tentorial bridge	ventral at precerbral pharynx	50	0bu6	54	pdlphy1, 2 (?)	23, 28 (?)	X
M. tentorio-pharyngalis posterior	te-ph(p)	tentorial bridge or posterior tentorial arm	ventral / ventrolateral at precerebral pharynx	52, 54 (?)	0ph2 (?)	55	pdlphy 3, 4, 2dlpphy (?)	28 (?)	X
M. cranio-pharyngalis anterior	cr-ph(a)	vertex	dorsal at postcerbral pharynx, behind supraoesophageal ganglion	51	0ph1	51	1dlpphy	27	X
M. cranio-pharyngalis posterior	cr-ph(p)	[posterolateral at cranium]	[dorsolateral at postcerebral pharynx]	51, 53 (?)	0ph1, 0ph3 (?)	52, 53	2dlpphy (?)	28 (?)	–
M. anularis cibarialis	an-ci	ring muscle fibers covering the prepharynx	–	67	0hy9	X (*)	rm	29	X
M. anularis pharyngalis	an-ph	ring muscle fibers covering the entire pharynx	–	68	0st1	X (*)	rm	29	X
M. longitudinalis pharyngalis	lo-ph	longitudinal muscle fibers stretching between the surface of the pharynx and an-ph	–	69	0st2	47	lm	n.a.	X
M. tentorio-scapalis anterior	te-sc(a)	anterior tentorial arm	anterior basal margin of scapus	1	0an1	3	abant2	5	X
M. tentorio-scapalis posterior	te-sc(p)	anterior tentorial arm	posterior basal margin of scapus	2	0an2	4	adant2	3	X
M. tentorio-scapalis lateralis	te-sc(l)	anterior tentorial arm	lateral basal margin of scapus	3	0an3	2	abant1	4	X (2 bundles)
M. tentorio-scapalis medialis	te-sc(m)	anterior tentorial arm	mesal basal margin of scapus	4	0an4	1	adant1	6	X
M. scapo-pedicellaris lateralis	sc-pe(l)	ventrolateral and ventromesal wall of scapus	ventral and ventrolateral basal margin of pedicellus	5	0an6	7, 8	adpde	n.a.	X (2 bundles)
M. scapo-pedicellaris medialis	sc-pe(m)	dorsal and ventromesal wall of scapus	dorsal at proximal margin of pedicellus	6	0an7	5, 6	abpde	n.a.	X (3 bundles)
M. cranio-mandibularis medialis	cr-md(m)	dorsal and lateral head capsule	adductor tendon of mandible	11	0md1	22	1admd	7	X

Table 1 continued.

Name	Abbrev.	Origin	Insertion	v. Kéler 1955	Wipfler et al. 2011	Hannemann 1956	Klemm 1966	Crichton 1957	present study
						Micropterix	*Rhyacophila*	*Phryganea*	*Philopotamus*
M. cranio-mandibularis lateralis	cr-md(l)	lateral at head capsule	abductor tendon of mandible	12	0md3	23	abmd	7	X
M. tentorio-mandibularis	te-md	anterior tentorial arm	mesally at inner wall of mandible	14	0md6	– (*)	2admd	–	X
M. hypopharyngo-mandibularis	hy-md	[hypopharyngeal sclerite]	[inner wall of mandible]	13	0md4	–	–	–	–
M. tentorio-cardinalis	te-cd	anterior tentorial arm	mesal process of ‚cardo' (cardo + basistipes)	17	0mx3	26	adcd	9	X
M. tentorio-stipitalis	te-st	anterior tentorial arm	mesal margin of ‚stipes' (dististipes)	18	0mx4	27	adst	–	X
M. cranio-cardinalis	cr-cd	postgena	proximolateral process of ‚cardo' (cardo + basistipes)	15	0mx1	24	J	8	X
M. cranio-stipitalis	cr-st	postgena	distal process of mesal stipital margin (dististipes)	16	0mx1	25	–	–	X
M. cranio-lacinialis	cr-lc	postgena	laterally at composite endite lobe of maxilla	19	0mx2	29	flcc	10	X
M. stipito-lacinialis	st-lc	[mesal at stipes]	[basal edge of lacinia]	20	0mx6	28	flcs	11	–
M. stipito-galealis	st-ga	[stipes]	[basal edge of galea]	21	0mx7	30	–	–	–
M. cardo-palpalis dorsalis	cd-mp(d)	proximomesal angle of ‚cardo' (cardo + basistipes)	dorsolateral at palpomere 1	–	–	–	lplp b	12, 13 (?)	X
M. stipito-palpalis dorsalis	st-mp(d)	mesally at proximal half of ‚stipes' (dististipes)	mesal at dorsal margin of palpomere 1	23	0mx10	31	lplp a	12, 13 (?)	X
M. stipito-palpalis ventralis / M. cardo-palpalis ventralis	st-mp(v) / cd-mp(v)	lateral at ‚cardo' (cardo + basistipes)	ventral basal margin of palpomere 1	22	0mx8	32	dplp	12, 13 (?)	X
M. palpo-palpalis maxillae primus medialis	mp1-mp2(m)	mesal wall of palpomere 1	dorsomesal at basal margin of palpomere 2	24 (?)	0mx12	33	X	X	X
M. palpo-palpalis maxillae primus lateralis	mp1-mp2(l)	mesal basal margin of palpomere 1	ventrolateral at basal margin of palpomere 2	24	0mx12	33	X	X	X
M. palpo-palpalis maxillae secundus	mp2-mp3	dorsal wall of palpomere 2	dorsolaterally at basal margin of palpomere 3	25	0mx13	34	X	X	X
M. palpo-palpalis maxillae tertius	mp3-mp4	dorsomesally at palpomere 3	ventromesally at basal margin of palpomere 4	26	0mx14	35	X	X	X
M. palpo-palpalis maxillae quartus	mp4-mp5	dorsomesal on distal half of palpomere 4	ventromesally at basal margin of palpomere 5	27	0mx15	36	X	X	X
M. hypopharyngo-salivarialis	hy-sa	lateral at ventral half of hypopharynx	proximally on the roof of the salivarium	37	0hy12	56, 57	–	–	X
M. intra-salivarialis	i-sa	[roof of salivarium]	[roof of salivarium]	37 (?)	–	–	1 (unpaired)	18	–
M. praemento-salivarialis	prm-sa	prementum	proximal half of the roof of the salivarium	38/39	0hy7, 0hy8 (?)	– (*)	2s	17	X
M. cranio-praementalis medialis	cr-prm(m)	postgena (together with cr-st)	mesally at distal part of prementum	30	0la6	39	1ablb, 2adlb	16	X (2 bundles)
M. cranio-praementalis lateralis	cr-prm(l)	mesal at postgena	lateral rim of palpiger	29	0la5	40	rst	16	X
M. submento-praementalis	smt-pmt	[submentum or gula]	[prementum]	28	0la8	41(*)	–	–	–
M. praemento-paraglossalis	prm-pgl	[basal edge of prementum]	[paraglossa]	31	0la11	37	–	–	–
M. praemento-glossalis	prm-gl	[mesally on prementum]	[glossa]	32	0la12	38	–	–	–
M. praemento-palpalis medialis	prm-lp(m)	mesally at dorsal face of prementum	lateral at proximal margin of palpomere 1	33	0la13	42	lplp	19, 20 (?)	X
M. praemento-palpalis lateralis	prm-lp(l)	proximolateral on palpiger	lateral at proximal margin of palpomere 1	34	0la14	43	dplp	19, 20 (?)	X
M. palpo-palpalis labii primus anterior	lp1-lp2(a)	lateral at the base of palpomere 1	anteriorly at the base of palpomere 2	35	0la16	44a (*)	X	X	X
M. palpo-palpalis labii primus posterior	lp1-lp2(p)	posteriorly at the base of palpomere 1	posteriorly at the base of palpomere 2	35 (?)	0la16	44b (*)		X	X
M. palpo-palpalis labii secundus	lp2-lp3	anterolaterally at the distal half of palpomere 2	laterally at the proximal margin of palpomere 3	36	0la17	–	X	X	X

Table 2. Overview of the morphological terminology applied to sclerites of the adult head capsule (cranium/'face') and to selected mouthpart structures (maxilla and labium) in Amphiesmenoptera compared with the generalized insect head (after BEUTEL et al. 2014). Abbreviations used: + = term used by the author as in the generalized insect head, – = structure not mentioned by the respective author (this does not indicate that the respective structure is absent in the taxon!).

	Generalized insect head		***Philopotamus*** **[Philopotamidae, Annulipalpia]**	***Rhyacophila*** **[Rhyacophilidae, 'Spicipalpia']**	***Stenophylax*** **[Limnephilidae, Integripalpia]**	***Phryganea*** **[Phryganeidae, Integripalpia]**	***Micropterix*** **[Micropterigidae, Lepidoptera]**
	BEUTEL et al. 2014		present study	KLEMM 1966	CHAUDONNERET 1990	CRICHTON 1957	HANNEMANN 1956
cranium	occiput		+	+	région occipitale	+	+
	vertex		+	—	—	—	+
	gena		+	+	+	+	+
	postgena		+	+	+	+	+
'face'	frons		frontopostclypeus	+	clypéofrons + aire postérieure du frons	frontoclypeus	+
	clypeus	postclypeus		clypeolabrum			+
		anteclypeus	anteclypeolabrum		clypéo-labre		
	labrum					+	+
maxilla	cardo		cardo + basistipes	+	+	+	+
	stipes	basistipes		+	+	+	+
		dististipes	+				
	lacinia		+	+	—	+	+
	galea		+	—	+	—	+
	postlabium		—	—	+	—	—
	postmentum		—	+		—	—
labium	submentum		—	—	—	—	+
	mentum		—	—	—	—	+
	prementum		+	+	+	+	+
	palpiger		+	—	+	distal labial sclerite	—
	paraglossa		endite lobes of labium	—	—	—	+
	glossa			—	—	—	+
	haustellar sclerites		—	+	+ (1, 2)	+ (1–3)	—

ed with the mandibular muscles. The thickest branch runs into the mandible closely accompanied by the extremely thin tentorio-mandibular muscle (te-md, see above) (Fig. 17E). The strong maxillary nerve (nmx in Fig. 18A,B) originates from the ventral side of the suboesophageal ganglion, distinctly behind the mandibular nerve. It runs into the maxilla innervating its muscles with very thin branches. The major part of the maxillary nerve forms the sensory branch, which enters the sensilla-rich palps. Shortly behind the maxillary nerve originates its almost equal thick labial counterpart (nla in Fig. 18A,B). It innervates the labial and salivary muscles. Analogous to the conditions of the maxilla, the main part of the labial nerve continue into the labial palp to receive information of the large array of different sensory setae (see above). A smaller branch (nh in Fig. 18A,B) is send to the sensilla of the haustellum.

3.15. Stomatogastric nervous system

The stomatogastric nervous system innervates the preoral and pharyngeal musculature. The moderately sized frontal ganglion is connected with anterior tritocerebral lobes by strong frontal connectives (fco in Figs. 17C, 18A). At the base of each connective originate the labrofrontal nerve, rapidly splitting up into two discrete fine branches. The very thin frontal nerves run downwards, merge each other after a short distance and proceed as an unpaired nervus frontalis (nfr in Fig. 18A) in front of the ganglion frontale downwards. The labral nerve (nlbr in Fig. 18A) runs more laterally, posterior to the ganglion frontale downwards sending branches to the clypeolabral dilator muscles. An unpaired nervus connectivus linking the frontal ganglion with the protocerebrum is absent. The nervus recurrens (nrec in Fig. 18A) originates from the hind face of the frontal ganglion and runs, between the pharyngeal ring musculature and the aorta, backwards below the brain and proceeds into the hypocerebral ganglion which forms together with the corpora cardiaca a somewhat diffuse structure. A thin occipital nerve (nocc in Fig. 18B) supplying the posterior part of the vertex, the occipital/postoccipital region, and the cervix originates from the posterior end of the suboesophageal ganglion, immediately above the cervical connectives.

3.16. Hypocerebral complex

Paired, diffuse neural glands (corpora cardiaca and corpora allata; together ccc in Fig. 16B,D) are situated adjacent to the dorsal face of the postcerebral pharynx and

the cephalic aorta with the comparatively small, rounded corpora cardiaca located directly behind the brain. They receive a thin and short nerve tract (nervus corpus cardiacus) from the brain. The considerably voluminous, elongated corpora allata are continuous with the corpora cardiaca and proceed into the neck region after receiving the nervus corpus allatum from the latter. A thin nerve originating laterally from the corpora allata connects it with the strong maxillary nerve.

3.17. Circulatory system

The cephalic aorta (ao in Figs. 16A, 17B) enters the head capsule through the alaforamen, directly dorsal to the pharynx. Its postcerebral part is voluminous but constricts rapidly before the passage through the circumoesophageal connectives. In front of the brain the aorta bents upwards and runs toward the area between the antennal sockets. It adheres to the posterior frontopharyngeal muscle (fr-ph(p)) (Fig. 17B) whose contractions may enhance the haemolymph flow. Between the antennae the aorta widens into a flat unpaired haemolymph sinus, reaching the median ocellus dorsally. Laterally, the sinus extends toward the antennal base, where it is continued as a thin vessel extending into the antenna (av in Fig. 17A). This antennal vessel runs, accompanied by a trachea, into the distal part of the flagellum. Specific dilator muscles of the aorta or the antennal sinus are absent. However, the thickened wall of the sinus lateral to the interantennal sulcus may contain muscle fibers and be contractile (muscle fibers could not be identified with certainty in histological sections at hand).

3.18. Tracheal system

Two pairs of main head tracheae (tra in Fig. 12B) pass through the alaforamen into the head capsule and flank the postcerebral pharynx dorsolaterally. The dorsal pair of stems split into two branches. One runs dorsolaterad and supplies the mandibular muscles whereas the second is almost exclusively associated with the brain and the antenna. The ventral stems proceed anterolaterad and split into numerous thin branches which supply the musculature of the ventral parts of the head capsule (mouthparts, cibarium, precerebral pharynx etc.).

3.19. Fat body

Fat body aggregations take approximately two thirds of the free lumen of the head (space not filled with musculature or the nervous system) (fb in Fig. 16A–D). They are only absent directly around the digestive, circulatory, nervous and tracheal systems. The entire antenna and the distal segments of the maxillary (3rd and following palpomeres) and labial palp (2nd and 3rd palpomere) are also free of fat body.

4. Discussion

4.1. Morphology & terminology

Morphological features of the skeleton and soft tissues of the adult head of *Philopotamus* are compared with conditions found in other trichopteran lineages (e.g., Rhyacophilidae, Phryganeidae), Lepidoptera and Mecoptera. The homology of trichopteran head sclerites and consequences for the terminology applied to head structures in caddisflies are discussed in detail (see also Table 2).

4.1.1. Frontopostclypeus

In *Philopotamus* externally visible demarcations between frons, clypeus and labrum are absent. In the generalized insect condition frons and clypeus are separated by a frontoclypeal strengthening sulcus (= epistomal sulcus of Snodgrass 1935), laterally demarcated by the anterior tentorial pits. Usually, the frontal region serves as attachment area of dilator muscles of the precerebral pharynx whereas the cibarial dilators are attached to the clypeus (see Snodgrass 1935, v. Kéler 1955). A frontoclypeal sulcus is absent in *Philopotamus* and *Hydropsyche*, as in *Phryganea* (Crichton 1957) and *Stenophylax* (Chaudonneret 1990). In contrast to Chaudonneret (1990), Demoulin (1960: 4, fig. 1; = clypeo-frontal sulcus) described a frontoclypeal sulcus in *Stenophylax* which originates from the anterior tentorial pits and curves dorsally toward the antennal bases. This sulcus is not homologous with a frontoclypeal sulcus due to the origin of pharyngeal dilators below the median ocellus which are attached to the frons in the generalized insect head (Snodgrass 1935). It rather resembles the frontogenal sulcus of Philopotamidae. This conclusion is also applicable to the dorsal demarcation of the 'clypeus' presented by Deoras (1943). A frontoclypeal sulcus is described for the leptocerid species *Ceraclea dissimilis* (Denis & Bitsch 1973: 422) and in *Rhyacophila* (Klemm 1966: 37 [= sulcus epistomalis]). In *Rhyacophila* a horizontal sulcus between the anterior tentorial pits is present but the dorsal cibarial dilator muscle is attached to the sulcus itself and also to the area above it (pers. obs.). Since the dilator muscles of the prepharyngeal tube are exclusively attached to the clypeus (see v. Kéler 1955) a homology of the horizontal sulcus in *Rhyacophila* to the frontoclypeal sulcus of the generalized insect head can be doubted.

Klemm (1966: fig. 11) described a membranous horizontal furrow ('querfaltige Membran') ventrally adjacent to the horizontal sulcus in *Rhyacophila*. A similar depression is present in many other trichopterans, as for instance in *Philopotamus* (hf in Fig. 1), *Phryganea* (Crichton 1957: unlabeled in fig. 26) and *Hydropsyche* (pers. obs). However, in contrast to *Rhyacophila* the horizontal furrow is not membranous in the other taxa. In *Philopotamus* the dorsal dilator muscles of the prepharyngeal tube originate from the head capsule in the area below

the anterior tentorial pits and also above the horizontal furrow which therefore also cannot be homologous with the frontoclypeal sulcus. Additionally, a ventral cibarial dilator muscle [cl-ci(v)] is attached below the horizontal furrow, rendering this structure as transclypeal. It separates the dorsal frontopostclypeus from a ventral anteclypeolabrum. Based on the origin sites of the cibarial dilator muscles Klemm (1966: 19) and Chaudonneret (1990: 78, fig. 175) correctly termed the area below the horizontal furrow in *Rhyacophila* and *Stenophylax*, respectively, as anteclypeolabrum (see Table 2). Klemm (1966) considered the area above the frontoclypeal sulcus as the frons and in consequence all attached muscles as dilators of the pharynx. There is no cibarial dilator muscle in *Phryganea* recorded as attaching below the horizontal furrow (Crichton 1957: fig. 26). Hence, Crichton (1957) regarded this lower region as a labrum and the area above the horizontal furrow the frontoclypeus; it accommodates the origins of both cibarial and pharyngeal dilator muscles. In accordance to Crichton's (1957) interpretation we conclude that the area above the anterior tentorial pits truly represents the frons in Philopotamidae and most other trichopterans but since the frontoclypeal sulcus is absent no clear border between frons and clypeus is present. Consequently, this composite formation has to be termed as frontoclypeus as proposed by Crichton (1957) and Chaudonneret (1990) (see Table 2). In *Micropterix* (Hannemann 1956) and other non-glossatan moths (Kristensen 2003) a frontoclypeal sulcus is well-developed but absent in all Glossata. Kristensen (2003: 43) linked the absence of a frontoclypeal sulcus to the loss of articulated mandibles in the post-pharate glossatan adults. This is also a plausible explanation for the loss of this structure in most trichopterans.

The frontopostclypeus of *Philopotamus* is dorsally subdivided by the interantennal sulcus which is also present in *Stenophylax* (Chaudonneret 1990: 78, fig. 172, stf) but is absent in *Rhyacophila* (pers. obs.; Klemm 1966) and *Phryganea* (Crichton 1957). A homology with the interantennal sulcus of some lepidopterans (Kristensen 2003: 41) is doubtful.

4.1.2. Anteclypeolabrum

The complete lack of the clypeo-labral articulation and of the fronto-labral muscles in all trichopteran species investigated so far impedes the exact delimitation of the labral and clypeal portions of the anteclypeolabrum. The combined loss of both features occurs in almost all insect taxa with an immobilized labrum (e.g., Friedrich et al. 2013; v. Kéler 1955: 722). A border between a well-sclerotized proximal part and a membranous apical area is distinctly developed in most trichopterans (e.g., Fig. 1, Klemm 1966: fig. 9). If it represents the anatomical clypeo-labral boundary remains uncertain due to the lack of associated muscles but seems to be at least possible since the epipharyngeal sclerite is laterally continuous with the anteclypeolabrum in this apical area. The proximal border of the structure described as labrum by Crichton (1957) for *Phryganea* (see above) is in fact the intraclypeal horizontal furrow. His interpretation was likely based on the absence of the ventral clypeo-cibarial dilator muscle. Crichton (1957: 61) assumed that the membranous tip in *Phryganea* is movable by an intrinsic muscle. Considering the sclerotization pattern of the labrum, this intrinsic muscle most likely allows only light movements or deformation of the membranous tip. It is most likely that it lifts only the epipharynx. Considering the absence of extrinsic labral muscles Crichton's interpretation has to be regarded as not supported. The interpretation of labrum and clypeus forming a composite anteclypeolabrum by Klemm (1966) and Chaudonneret (1990) is comparable with the condition found in Philopotamidae. In the ground plan of Lepidoptera the labrum is moved by paired frontal retractor muscles and is proximally well delimited by a clypeo-labral hinge (Kristensen 2003).

4.1.3. Gena and occiput

The gena is anteriorly delimited from the frontopostclypeus by the distinct frontogenal sulcus. The latter extends from the ventral margin of the circumantennal sulcus toward the anterior tentorial pit in Trichoptera; the corresponding internal ridge is of variable size (Klemm 1966; Neboiss 1991). In Lepidoptera a frontogenal sulcus (= laterofacial sulcus of Kristensen 2003) is usually well-developed in the glossatan lineages but joins the circumantennal sulcus dorsolaterally. It has been shown in other insect groups that the length and connections of the circumantennal and frontogenal sulci can strongly vary even between closely related taxa, depending on other anatomical features (see Klass & Eulitz 2007). A well-sclerotized clypeogenal sulcus as described by Crichton (1957) for *Phryganea* could not be observed in *Philopotamus* and is also absent in *Rhyacophila* (Klemm 1966: 37).

A typical feature of the trichopteran head capsule is the elongation of the ventral edge of the gena forming a subgenal process. This process is also a typical feature of Mecoptera (Mickoleit 1971; Friedrich et al. 2013) and basal lepidopterans (Kristensen 2003). As described for *Philopotamus* the postgena is continuous with the occiput in all other investigated trichopterans (Klemm 1966; Crichton 1957) while it is distinct in *Micropterix* (Hannemann 1956) and other lepidopteran lineages (Kristensen 2003). Frontal and coronal sulci are generally present in Trichoptera (*Philopotamus*, *Hydropsyche*, *Phryganea* [pers. obs.], *Rhyacophila* [= sulcus mediocranialis of Klemm 1966], *Stenophylax* [Demoulin 1960]). The postfrontal sulcus described for *Philopotamus* and *Stenophylax* (Demoulin 1960) are most probably homologues to the medio-lateral reinforcement lines described by Klemm (1966: 8) and the postinterocellar sulcus described by Hannemann (1956) for *Micropterix*. These sulci are completely absent in *Phryganea* (pers. obs.). Interocellar sulci occurring in some lepidopteran lineages (Kristensen 2003) are not known from Trichoptera.

4.1.4. Tentorium

The tentorium of Philopotamidae is characterized by extremely reduced dorsal tentorial arms and a well-developed corpotentorium resulting in an X-shaped configuration of the anterior and posterior tentorial arms. Full developed dorsal tentorial arms appear as a characteristic feature of the integripalpian lineage Plenitentoria (e.g., Phryganeidae [Crichton 1957], Limnephilidae: *Stenophylax* [Demoulin 1960], Goeridae, and Brachycentridae [Neboiss 1991]). They are remarkably weak developed or completely absent in Annulipalpia (see Neboiss 1991), Rhyacophilidae (Klemm 1966) and also in some Integripalpia (e.g., Brevitentoria: Sericostomatidae [see Neboiss 1991]). A similar pattern of weakly and well-developed dorsal arms is found in Lepidoptera (see Kristensen 2003: 44). The X-shaped configuration of the tentorium can also be found in Hydropsychidae (Neboiss 1991). In most other lineages of Trichoptera (e.g., Rhyacophilidae, Glossosomatidae, Psychomyiidae, Leptoceridae) it is H- or Π-shaped (Neboiss 1991) as in Lepidoptera-Micropterigidae (Kristensen 2003). Therefore, a Π-shaped configuration is added to the trichopteran ground plan. The presence of a plate-like corpotentorium in Philopotamidae is a potential autapomorphy of the group (see Neboiss 1991). Similar conditions present in the agathiphagid and heterobathmiid lepidopterans (Kristensen 2003) are very likely convergently developed, because all spicipalpian representatives show other configurations (Neboiss 1991). A large, heavily sclerotized laminatentorium occurs in several not closely related groups (e.g., Hydropsychidae (Annulipalpia), Hydrobiosidae (spicipalpians), and Leptoceridae (Integripalpia) [Neboiss 1991]).

4.1.5. Setal warts

A specific feature of the trichopteran head is the presence of numerous, bulged setal warts equipped with numerous large trichoid sensilla. The homology of these areas is uncertain due to the high variability in presence and location in different trichopteran lineages (see Oláh & Johanson 2007). In previous descriptions these structures were often neglected or at least insufficiently described (see Crichton 1957; Klemm 1966). Detailed comparative studies are not available.

4.1.6. Photoreceptors

The compound eye of Philopotamidae is irregularly covered by a few interommatidial setae. The number of setae as well as their distribution on the compound eye varies among caddisfly families (see Schmid 1998), and can even be species specific (pers. obs.: *Philopotamus* and *Wormaldia* [Philopotamidae]). Neither Crichton (1957) nor Klemm (1966) mentioned the presence of interommatidial setae in Rhyacophilidae and Phryganeidae, respectively, although they are visible in light microscopy and are commonly present in Trichoptera (pers. obs.) and in Lepidoptera (Kristensen 2003).

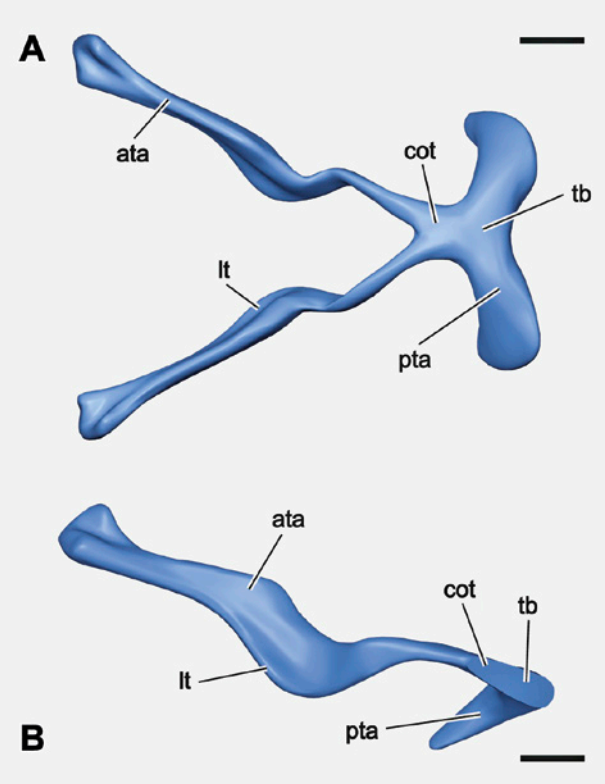

Fig. 14. *Philopotamus ludificatus* McLachlan, 1878: tentorium, 3D-reconstruction based on µCT data. **A**: dorsal view, **B**: sagittal section (dorsal tentorial arm not shown; see Fig. 17C). — ***Abbreviations***: ata – anterior tentorial arm, cot – corpotentorium, lt – laminatentorium, pta – posterior tentorial arm, tb – tentorial bridge. (Scale bars: 100 µm)

Furthermore, in *Philopotamus* the ommatidial cornea shows a specific surface texture of rounded corneal nipples (absent along the interommatidial space), a common feature of the insect compound eye in order to reduce reflection artifacts (Bernhard & Miller 1962; Bernhard et al. 1970). These extremely minute structures are not mentioned by Crichton (1957) and Klemm (1966), likely due to technical constraints. The structure of corneal outgrowths varies among insects from knob-like nipples to parallel sulci (Meyer-Rochow & Stringer 1993). Evidence for the presence of corneal nipples of the knob-like type among 15 different caddisfly families (including Philopotamidae) was provided by Bernhard et al. (1970). A textured surface of the ommatidial cornea is also commonly found in Lepidoptera (Kristensen 2003) and Mecoptera (Bernhard et al. 1970).

Three ocelli are present in *Philopotamus*, *Rhyacophila* (pers. obs.; Klemm 1966) and *Phryganea* (pers. obs.; Crichton 1957) but the occurrence of ocelli is quite variable among trichopteran lineages (see Malicky 1973). This is also true for the lateral ocelli in Lepidoptera; the median one is reduced in all groups (Kristensen 2003).

Histological sections show that the ocelli in *Philopotamus* have a comparatively thin corneal lens of the convexo-concave type (after Hallberg & Hagberg 1986) whereas the haemocoelic space is voluminous (pers.

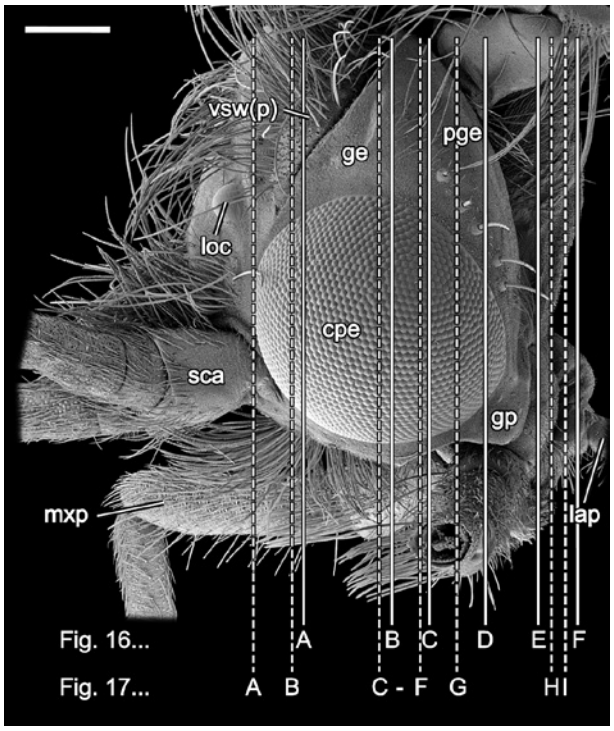

Fig. 15. *Philopotamus ludificatus* McLachlan, 1878: head, SEM image. **A**: lateral view with section planes of Figs. 16 (continuous lines) and 17 (dashed lines) marked. — ***Abbreviations***: cpe – compound eye, ge – gena, gp – subgenal process, lap – labial palp, loc – lateral ocellus, mxp – maxillary palp, pge – postgena, sca – scapus, vsw(p) – posterior setal wart of vertex. (Scale bar: 200 μm)

obs.; EHNBOM 1948). A similar condition was described for limnephilids by EHNBOM (1948) and HALLBERG & HAGBERG (1986), and is also found in the micropterigid moths (EHNBOM 1948; KRISTENSEN 2003). The corneal lens is much thicker (biconvex type), and underlain by an epidermal layer in phryganeids (pers. obs.: *Phryganea*; EHNBOM 1948; HALLBERG & HAGBERG 1986). This is also the common condition in most heteroneuran lepidopterans (EHNBOM 1948; KRISTENSEN 2003). Eriocraniidae are different in having the haemocoelic space filled up by a multicellular formation (see KRISTENSEN 2003) not known from any other amphiesmenopteran insect.

An imaginal stemma consisting of numerous heavily pigmented retinula cells is attached to the optical lobe in all investigated Trichoptera (pers. obs.: *Philopotamus*, *Rhyacophila*; EHNBOM 1948; HAGBERG 1986). Initially, this formation which represents a remnant of the larval eyes in the adult stage was described for phryganeids by EHNBOM (1948). Its appearance is variable on family level. Usually each stemma consists of numerous retinula cells associated to at least one crystalline body (see EHNBOM 1948; HAGBERG 1986: fig. 2). They are common features of the endopterygote adult head and can be found in various insect groups (i.e., Lepidoptera [HAGBERG 1986; KRISTENSEN 2003]; Megaloptera [*Sialis*, EHNBOM 1948]). In Lepidoptera the imaginal stemma is located inside the lobus opticus whereas it is found outside, behind the optic lobe in caddisflies and most other holometabolous insect orders (e.g., Megaloptera, Neuroptera, and Mecoptera, see EHNBOM 1948). HAGBERG (1986) concluded that these sensory organs are associated with cranial areas of glabrous, translucent cuticle. A small glabrous, bulged field near the lateral ocelli in *Philopotamus* might be comparable. If this structure and the stemma are functionally correlated cannot be assessed with final certainty because they are distinctly separated in *Philopotamus*.

4.1.7. Antenna

The length of the antenna varies remarkably among Trichoptera. In most groups (including Philopotamidae and Limnephilidae) it is as long as the forewing. But it is considerably shorter in Hydroptilidae (app. half of length of forewing) or extremely long as in Leptoceridae (app. three times longer than forewing length), respectively.

→ Fig. 16. *Philopotamus ludificatus* McLachlan, 1878: head, cross-sections. **A**–**F**: Cross-sections in dorsal-ventral sequence. — ***Abbreviations***: abte – tendon of abductor muscle of mandible (M. cranio-mandibularis lateralis), acl(d) – distal part of anteclypeolabrum, acl(p) – proximal part of anteclypeolabrum, adte – tendon of adductor muscle of mandible (M. cranio-mandibularis medialis), an-ci – M. anularis cibarialis, an-ph – M. anularis pharyngalis, ao – aorta, ata – anterior tentorial arm, br – brain, ccc – corpora cardiaca & corpora allata complex, cd-mp(d) – M. cardo-palpalis dorsalis, cd-mp(v) – M. cardo-palpalis ventralis, cl-ci(d) – M. clypeo-cibarialis dorsalis, cl-ci(v) – M. clypeo-cibarialis ventralis, cl-eph(l) – M. clypeo-epipharyngalis lateralis, coc – circumoesophageal commissure, cos – circumocular sulcus, cpe – compound eye, cr-lc – M. cranio-lacinialis, cr-md(l) – M. cranio-mandibularis lateralis, cr-md(m) – M. cranio-mandibularis medialis, cr-ph(a) – M. cranio-pharyngalis anterior, cr-prm(l) – M. cranio-praementalis lateralis, cr-prm(m) – M. cranio-praementalis medialis, cr-st – M. cranio-stipitalis, dol – deutocerebral olfactory lobe, eph – epipharynx, fb – fat body, fgs – frontogenal sulcus, fsal – floor of salivarium, fr-ph(p) – M. fronto-pharyngalis posterior, ga – galea, gp – subgenal process, hst – haustellum, is – immaginal stemma, md(s) – mandibular sclerite, mp1-mp2(l) – M. palpo-palpalis maxillae primus lateralis, mp1-mp2(m) – M. palpo-palpalis maxillae primus medialis, mp2-mp3 – M. palpo-palpalis maxillae secundus, nla – labial nerve, nmx – maxillary nerve, ocs – occipital sulcus, ol – optical lobe of protocerebrum, pch – precerebral pumping chamber, ph – pharynx, poc – preoral cavity, ppg – palpiger, ppt – prepharyngeal tube, prm-lp(l) – M. praemento-palpalis lateralis, prm-lp(m) – M. praemento-palpalis medialis, prm-sa – M. praemento-salivarialis, rsal – roof of salivarium, sit – sitophore plate, soeg – suboesophageal ganglion, st-mp(d) – M. stipito-palpalis dorsalis, tb – tentorial bridge, te-cd – M. tentorio-cardinalis, te-ph(a) – M. tentorio-pharyngalis anterior, te-ph(p) – M. tentorio-pharyngalis posterior, te-sc(a) – M. tentorio-scapalis anterior, te-sc(l) – M. tentorio-scapalis lateralis, te-sc(m) – M. tentorio-scapalis medialis, te-sc(p) – M. tentorio-scapalis posterior, te-si – M. tentorio-sitophorialis, te-st – M. tentorio-stipitalis, tra – trachea, I, and II – number of palpomere of maxillary palp. (Section planes marked in Fig. 15, continuous lines) (Scale bars: A–E: 250 μm; F: 100 μm)

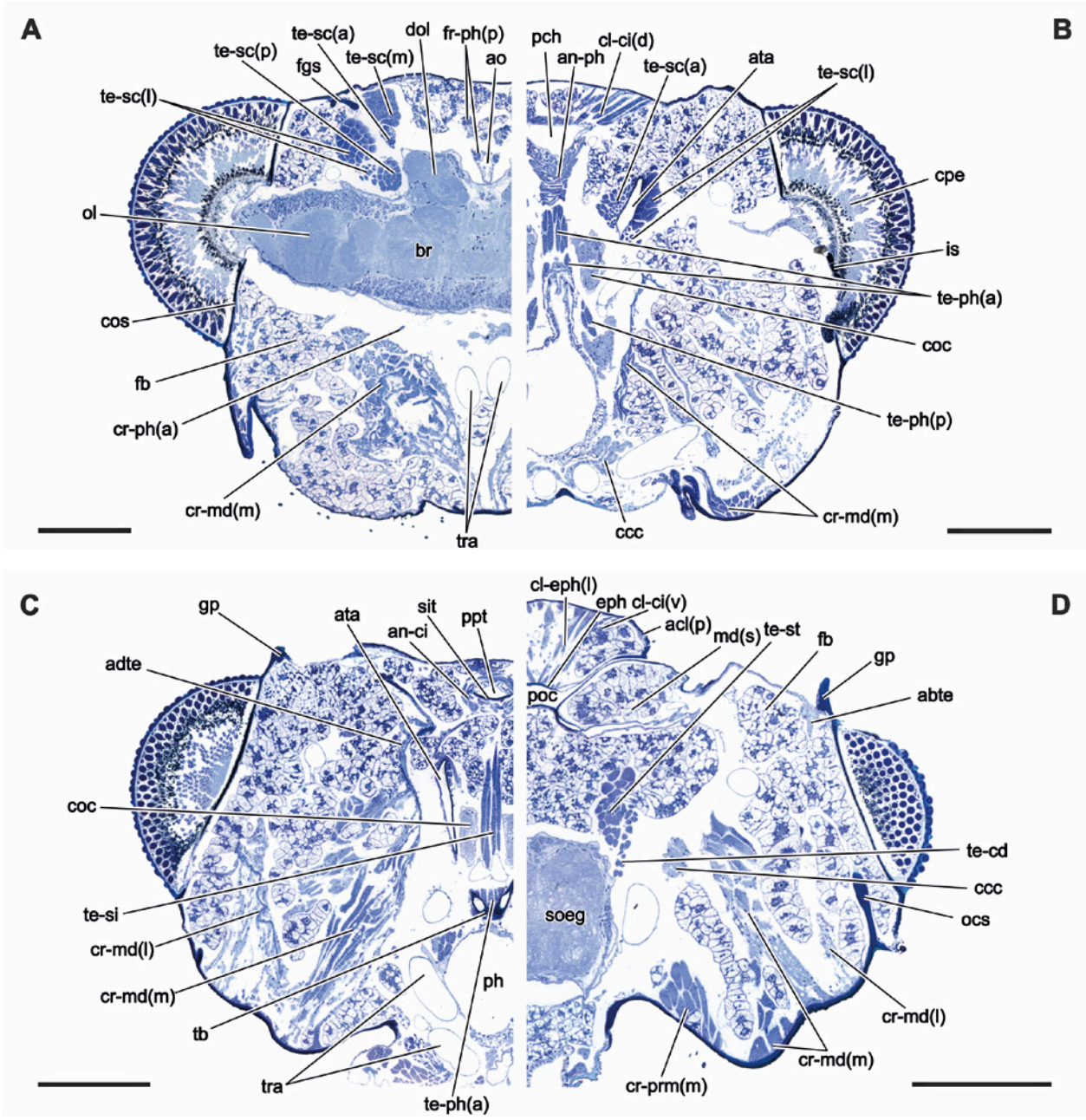
A
te-sc(p)
te-sc(a)
dol
fr-ph(p)
fgs
te-sc(m)
ao
te-sc(l)
ol
br
cos
fb
cr-ph(a)
cr-md(m)
tra
B
pch
an-ph
cl-ci(d)
te-sc(a)
ata
te-sc(l)
cpe
is
te-ph(a)
coc
te-ph(p)
cr-md(m)
ccc
C
gp
ata
sit
ppt
an-ci
adte
coc
te-si
cr-md(l)
cr-md(m)
tb
tra
ph
te-ph(a)
D
cl-eph(l)
eph cl-ci(v)
acl(p)
md(s)
te-st
fb
gp
poc
abte
te-cd
ccc
ocs
soeg
cr-md(l)
cr-md(m)
cr-prm(m)
E
ll
mp2-mp3
mp1-mp2(m)
acl(d)
cr-lc
mp1-mp2(l)
ga
l
nmx
prm-sa
rsal
fsal
prm-lp(l)
cd-mp(v)
st-mp(d)
cd-mp(d)
te-st
cr-st
cr-prm(m)
cr-prm(l)
F
ga
hst
ppg
prm-lp(m)
nla

→ **Fig. 17.** *Philopotamus ludificatus* McLachlan, 1878: head, cross-sections in dorsal-ventral sequence. **A**: base of antenna with antennal ampulla, **B**: head aorta accompanied by bundles of posterior fronto-pharyngeal muscle (marked by arrow) in front of the brain, **C**: precerebral pharynx at level of the ganglion frontale, **D**: mid part of the anterior tentorial arm with origin of tentorio-antennal muscles and M. tentorio-mandibularis (extremely thin), **E**: region short distance ventrad from (D) with M. tentorio-mandibularis accompanied by mandibular nerve, **F**: prepharyngeal tube below the frontal ganglion with dorsal margin of the sitophore plate, **G**: sitophore plate short distance below (F), **H**: cervical region with salivary glands, **I**: proximal part of salivarium. — ***Abbreviations***: aa – antennal ampulla, an-ci – M. anularis cibarialis, an-ph – M. anularis pharyngalis, ao – aorta, ata – anterior tentorial arm, av – antennal vessel, br – brain, cco – cervical connective, cl-ci(d) – M. clypeo-cibarialis dorsalis, coc – circumoesophageal commissure, cr-prm(m) – M. cranio-praementalis medialis, cvm – cervical membrane, dol – deutocerebral olfactory lobe, dta – dorsal tentorial arm, fb – fat body, fco – frontal connective, fg – ganglion frontale, fr-ph(p) – M. fronto-pharyngalis posterior, hy-sa – M. hypopharyngo-salivarialis, ias – interantennal sulcus, nmd – mandibular nerve, ph – pharynx, ppt – prepharyngeal tube, sal – salivarium, sc-pe(m) – M. scapo-pedicellaris medialis, sd – salivary duct, sg – salivary gland, sit – sitophore plate, te-md – M. tentorio-mandibularis, te-ph(a) – M. tentorio-pharyngalis anterior, te-ph(l) – M. tentorio-pharyngalis lateralis, te-sc(a) – M. tentorio-scapalis anterior, te-sc(l) – M. tentorio-scapalis lateralis, te-sc(m) – M. tentorio-scapalis medialis, te-sc(p) – M. tentorio-scapalis posterior, te-si – M. tentorio-sitophorialis, tra – trachea, trc – tritocerebral commissure, tri – tritocerebrum. (Section planes marked in Fig. 15, dashed lines) (Scale bars: 100 μm)

The antenna bears numerous sense organs which mainly function as chemical receptors. These sense organs vary considerably in their shape among Trichoptera (see Faucheux 2004; Melnitsky & Ivanov 2011) and Lepidoptera (Kristensen 2003; Faucheux 2004). In Philopotamidae and Stenopsychidae the number of fungiform pseudoplacoid sensilla along the antenna is remarkably high (pers. obs.) but this type of sense organs can be found regularly among Trichoptera (Melnitsky & Ivanov 2011).

In Trichoptera the antenna (i.e., the scapus) is moved by four extrinsic muscles originating mainly from the tentorium (e.g., in Philopotamidae, Limnephilidae [pers. obs.]; Phryganeidae [pers. obs.; Crichton 1957], and Rhyacophilidae [Klemm 1966]) or with at least one bundle from the cranium (e.g., in Polycentropodidae and Hydropsychidae [pers. obs.]) but data on this potentially phylogenetically valuable character complex is quite limited. This corresponds with the number and origin pattern of extrinsic antennal muscles in Lepidoptera. In contrast, only three or two are present in Mecoptera (e.g., Friedrich et al. 2013). The remaining parts of the antenna are moved by two intrinsic muscles arising from the scapus with several bundles. Maybe these bundles belong to more than two muscles as in the ground plan condition of Lepidoptera (Kristensen 2003) but with the data at hand the homology of these muscles remains unclear and should be investigated in detail for a larger set of taxa.

4.1.8. Mandible

The mandibular sclerite of *Philopotamus* is moderately sized and sclerotized as it is in *Rhyacophila* (Klemm 1966). In Integripalpia it is less sclerotized and often almost vestigial (*Phryganea* [Crichton 1957]; *Stenophylax* [Demoulin 1960; Chaudonneret 1990: 77, fig. 172]). The conditions of the mandibular musculature distinctly differ in the trichopteran species studied so far. While the adductor muscle is strongly developed in annulipalpians (pers. obs.) and in *Rhyacophila* (Klemm 1966; pers. obs.), it is comparatively small in *Phryganea* (Crichton 1957: 60, fig. 25).

In spite of the remarkable differences between the major groups of caddisflies in size of the mandibular sclerite, sclerotization and musculature development in all post-pharate imagines lack any cranio-mandibular articulations (pers. obs.; Chaudonneret 1990; Kristensen 1997). Hence, the mandible is most likely never functional for the processing of solid food (see also Crichton 1957). As highlighted by Hinton (1946) the mandibular muscles of adult endopterygote insects with decticous pupae operate the pupal mandibles when the pharate imago hatches from the cocoon; in the post-pharate stage of caddisflies and glossatan moths they are functionless and therefore may become atrophied. This might be a possible explanation for descriptions of differently sized mandibular muscles in Trichoptera (Crichton 1957; Klemm 1966). However, a detailed documentation of the development of the mandibular musculature during aging of the imagines is not available.

4.1.9. Preoral cavity and mouth opening

The interpretations of the facial areas (see above) mainly depend on the demarcation of the anatomical mouth opening. After Snodgrass (1935) the border between the prepharyngeal tube (= cibarium) and the pharynx is usually marked by the frontal ganglion. Accordingly, in *Philopotamus* all muscles inserting below the frontal ganglion are termed prepharyngeal (= cibarial) dilators whereas muscles attached above the frontal ganglion are regarded as pharyngeal dilators. The prepharyngeal tube is encircled by ring musculature and clearly contributes to a large cibarial-pharyngeal pumping chamber which represents a composite structure in *Philopotamus*. Klemm (1966) regarded this part as the cibarium and determined the morphological mouth opening at the anterior border of the pharyngeal ring musculature. He considered the muscles above this border either as cibarial dilators or as pharyngeal dilators depending on the origin site below or above the horizontal sulcus (his sulcus epistomalis, see above). It seems not appropriate to separate the preoral cavity into a proximal cibarium enclosed

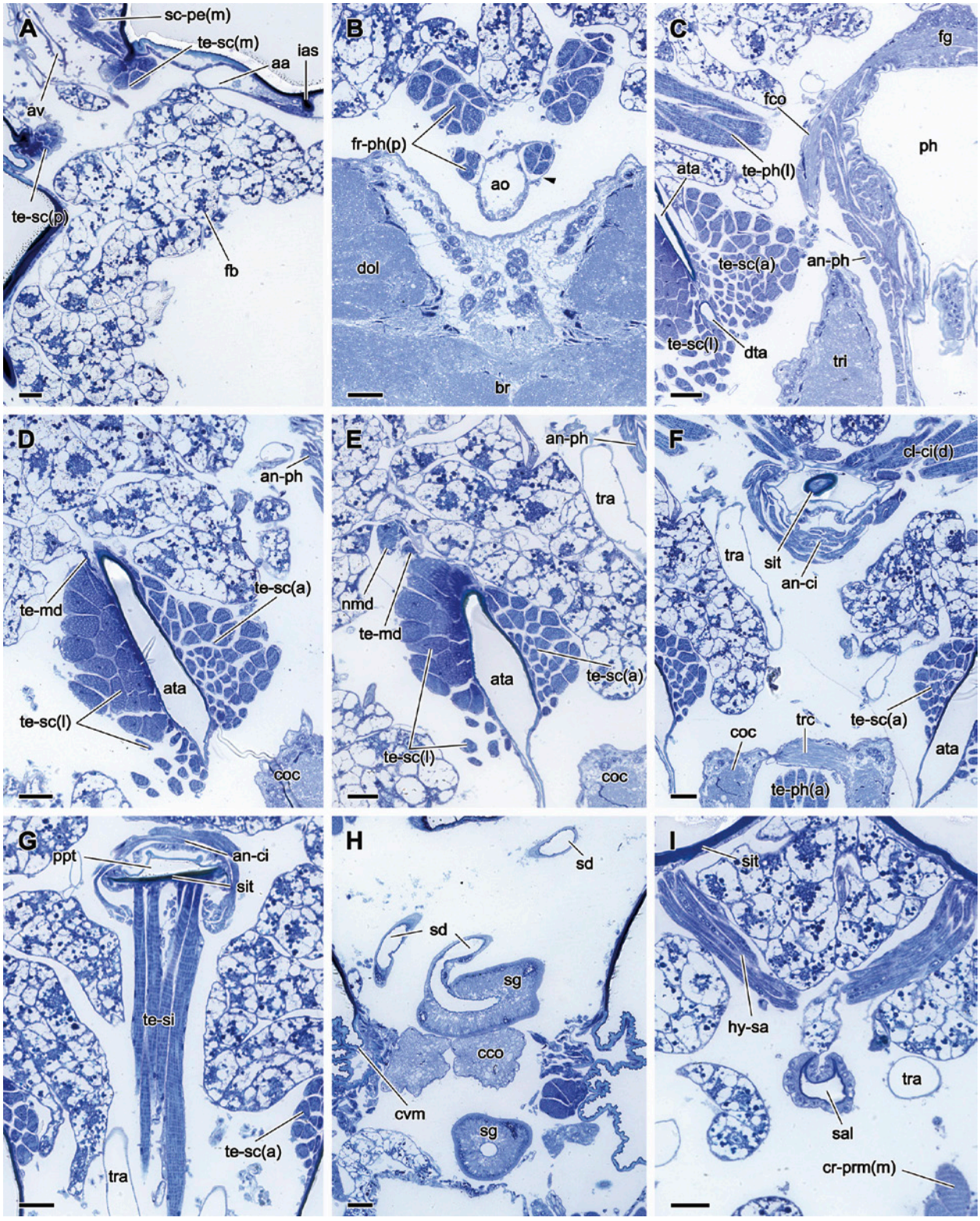

by pharyngeal circulatory musculature and a distal part without ring musculature as proposed by KLEMM (1966) since the sitophore plate (i.e. the sclerotized section of the hypopharynx) is a continuous structure and clearly forms the bottom of the composite pumping chamber. In lepidopterans the ring musculature is located behind the frontal ganglion but the roof of the cibarium is only covered by semicircular and longitudinal muscle fibers (KRISTENSEN 2003). This semicircular type of cibarial pump musculature is so far not known from any trichopteran species.

The surface of the sitophore plate lacks any chemoreceptors in *Philopotamus* and the sparse literature (CRICHTON 1957; KLEMM 1966) gives no evidence that sensilla are present along the floor of the preoral cavity in any other trichopteran. In Lepidoptera the sitophore is usu-

ally equipped with numerous chemoreceptors (Nielsen & Kristensen 1996).

4.1.10. Maxilla

In Trichoptera the base of the maxilla is formed by one sclerite which is intermitted by a transstipital sulcus. This sulcus was usually misinterpreted as a border between 'cardo' and 'stipes' (e.g., Crichton 1957; Matsuda 1965; Klemm 1966). In Lepidoptera the proximal maxillary sclerite (apparent 'cardo') is subdivided into two sections by an internal sulcus and delimited from the stipes (dististipes) by a small membranous area (Hannemann 1956: 191; Kristensen & Nielsen 1979: 117). In *Philopotamus* as in *Rhyacophila* (Klemm 1966) no membranous subdivision of the basal maxillary sclerite could be observed. A strong horizontal sulcus delimits the apparent cap-like cardo and the stipes. Intriguingly, a couple of extrinsic muscles of the maxillary palp originate from the putative cardo. A cardo-palpal muscle is not present in any other insect group (see e.g., Wipfler et al. 2011; v. Kéler 1955) and therefore it is more plausible to assume that these muscles are homologues to the stipito-palpal muscle of the insect ground plan (e.g., Snodgrass 1935: 143). The insertion of these palpal muscles to the basalmost maxillary piece in both amphiesmenopteran lineages led to the interpretation that this sclerite represents a combination of cardo and basistipes (Hinton 1958; Kristensen & Nielsen 1979; Kristensen 2003). Accordingly, the horizontal sulcus present in Trichoptera does not demarcate the border between 'cardo' and 'stipes' as suggested by several authors (e.g., Klemm 1966; Chaudonneret 1990), but forms a transstipital border between a basal piece (cardo + basistipes) and the dististipes. The inclusion of a cardinal portion in the basal piece is well proven by the presence of the cranio-cardinal muscle (cr-ca).

In Philopotamidae and the spicipalpian families Rhyacophilidae (Klemm 1966) and Glossosomatidae (Chaudonneret 1990: *Agapetus*) the maxilla bears two proximally fused inner appendages: a distinct, flattened outer lobe and a comparatively small, sclerotized inner lobe. In *Philopotamus* this composite structure is moved by a cranial flexor muscle, which might be homologous to the cranio-lacinial muscle of generalized insects (v. Kéler 1955: M.19). Additionally, Klemm (1966: 18) described for Rhyacophilidae a stipito-lacinial muscle inserting at the small inner lobe. This muscle is absent in Philopotamidae. In Integripalpia (e.g., Phryganeidae [Crichton 1957: 63]) the maxillary endite lobe is a single structure without any subdivision, but both the cranio-lacinial and the stipito-lacinial muscle are present. This led several authors to regard this clearly composite lobe of Trichoptera as the lacinia, an interpretation which cannot be accepted considering the conditions in basal representatives. Furthermore, as discussed by Kristensen (2003: 53) and Beutel et al. (2014: 21) the lacinia is usually distinctly stronger sclerotized and less equipped with sensilla (chemoreceptors) than the galea. Therefore, it seems also appropriate to consider the membranous outer maxillary lobe which bears numerous basiconic sensilla as the galea as suggested by Chaudonneret (1990: 80) and only the small inner piece as the remnants of the lacinia, which is largely (e.g., Rhyacophilidae) or completely incorporated (e.g., Phryganeidae) into the outer lobe which therefore should be regarded as a galeolacinia.

4.1.11. Haustellum

The origin of the trichopteran haustellum was a subject of controversy for decades. Several authors homologized the whole haustellum with the fused inner and outer lobes of the labium, i.e., the ligula (Lucas 1893; Deoras 1943; Despax 1951; Handlirsch & Beier 1936). The small inner labial lobes present in annulipalpians (pers. obs.) and *Rhyacophila* (Klemm 1966) most likely represent remnants of these labial appendages. This renders the hypothesis of the haustellum being a modified ligula very unlikely.

A second hypothesis favored by Cummings (1914), Tillyard (1923) and Klemm (1966) considered the haustellum as a ventral outgrowth of the hypopharynx. Indeed, the salivary orifice is located on the lower anterior (e.g., *Philopotamus*) or posterior (e.g., *Stenophylax* [Chaudonneret 1990]) surface of the haustellum. Usually it marks the border between the hypopharynx and the labium (Moulins 1971; Beutel et al. 2014: 22). Therefore, at least the upper anterior part of the haustellum must be of hypopharyngeal derivation.

Crichton (1957) showed that the haustellum in *Phryganea* is innervated by a branch of the mandibular nerve but also receives a branch of the labial nerve. He concluded that the lower section of the haustellum is most likely formed by the labium whereas the hypopharynx contributed to the upper part of this composite structure. The investigation of *Philopotamus* showed that the haustellum as well as the salivarium are only innervated by branches of the labial nerve.

In conclusion a composite nature of the haustellum seems to be well supported by the location of the salivary orifice and by its innervation by different nerve tracts. However, the latter seems not to be consistent throughout all trichopteran lineages and needs further detailed research.

In *Philopotamus* and *Rhyacophila* (pers. obs.) the haustellum is a completely membranous, highly flexible structure distinctly separated from the sclerotized prementum. Sclerites are absent. Small, distinctive basal haustellar sclerites were described for some integripalpians by Crichton (1957) and Chaudonneret (1990). These sclerites serve as attachment areas of the labial palp muscles and represent most likely derivatives of the prementum in the generalized insect condition (e.g., Snodgrass 1935: 147).

The fine structure of the haustellar surface varies considerably between Annulipalpia and Rhyacophilidae on one hand and Integripalpia on the other. The upper surface of the haustellum in *Philopotamus* and *Rhyacophila* (pers. obs.; Klemm 1966) is densely covered by numerous irregularly distributed, multibranched microtrichia. The

corresponding microtrichia in Phryganeidae and Limnephilidae are arranged in rows forming a regular system of channels on the surface of the haustellum (Crichton 1957, 1989, 1992; Chaudonneret 1990) which is absent in most annulipalpian groups (Crichton 1992).

4.1.12. Salivarium

In all Trichoptera investigated so far the salivarium orifice is located on the surface of the haustellum, distinctly below the preoral cavity. In *Philopotamus* it is located on the anterior surface of the haustellum but on its hind face in *Rhyacophila* (Klemm 1966) and Integripalpia (Crichton 1957; Chaudonneret 1990). In Lepidoptera and most other endopterygote insects the salivary orifice is located at the distal end of the hypopharynx, and distinctly opens into the preoral cavity (Kristensen 2003).

In Trichoptera the salivarium forms a longitudinal, sclerotized channel with U-shaped cross-section. A pair of extrinsic dilator muscles (M. hypopharyngo-salivarialis and M. praemento-salivarialis) inserts on its dorsal wall in *Philopotamus* and *Rhyacophila*. In contrast, in other pterygote insects M. praemento-salivarialis inserts ventrally on the floor of the salivarium (e.g., v. Kéler 1955; Snodgrass 1935; Röber 1942 [Megaloptera]; Kristensen 2003 [Lepidoptera: Acanthopteroctetidae]). Therefore, it seems to be at least possible that the sclerite on which these muscles originate is a derivate of the hypopharyngeal suspensorium of the generalized insect condition and hence the muscle may constitute a displaced bundle of M. hypopharyngo-salivarialis. Extrinsic dilators of the salivarium originating from the prementum are absent in most mecopterid lineages like Lepidoptera (with the exception of Acanthopteroctetidae; Kristensen 2003: 60) and Mecoptera (e.g., Grell 1938; Friedrich et al. 2013). Furthermore, in *Phryganea* (Crichton 1957), *Rhyacophila* (Klemm 1966), and *Merope* (Mecoptera [Friedrich et al. 2013]) the hypopharyngeal dilator of the salivarium is also absent.

In most trichopterans (Rhyacophilidae [pers. obs., Klemm 1966]; Phryganeidae [Crichton 1957] and Limnephilidae [Chaudonneret 1990]) a strong longitudinal muscle along the roof of the salivarium is present. This intrinsic salivary muscle is absent in Philopotamidae and other holometabolan lineages (Röber 1942 [Neuropterida: Megaloptera]; Kristensen 2003 [Lepidoptera]; Schneeberg & Beutel 2011 [Diptera]). Instead a well-developed extrinsic dilator muscle originates from the floor of the hypopharynx (hy-sa) in the annulipalpian groups or from the premental ligula in other holometabolan taxa (e.g., Megaloptera [Röber 1942]). As all trichopterans with intrinsic longitudinal salivary muscles lack the extrinsic hypopharyngeal muscle it is logical to assume the potential homology of these muscles of the salivary roof.

4.1.13. Labium

The labium of the generalized insect head is composed of a proximal postmentum and a distal prementum which bears the labial palps and the inner endite lobes (e.g., Beutel et al. 2014). In Lepidoptera the labium is usually separated into three distinct sclerotized areas (postlabium, proximal prelabium and prementum) distinguishable either by membranous segregation or by muscle insertion (see Kristensen 2003). In Philopotamidae both elements are largely fused forming a weakly sclerotized labial plate bearing the labial palps. In contrast, Crichton (1957), Klemm (1966), and Chaudonneret (1990) described the presence of distinct labial sclerites in Integripalpia and Rhyacophilidae (see Table 2). Unfortunately, the identification of these structures is complicated by the absence of a postlabio-premental muscle in all trichopterans investigated so far. Hence, a pre- or postmental derivation of these labial sclerites cannot be proven with any certainty. For a thorough interpretation of these structures comprehensive studies are needed.

The labium bears small inner lobes in all annulipalpians (*Philopotamus*, *Hydropsyche* [pers. obs.; Crichton 1957]) and in Rhyacophilidae (pers. obs.; Klemm 1966), whereas these are absent in Integripalpia (e.g., Crichton 1957; Chaudonneret 1990). The formation of a 'ligula' (fused glossae after Kristensen 2003: 57) is a common feature in Lepidoptera. Distinct paraglossae retained only in Micropterigidae (Kristensen 2003). In Trichoptera the inner lobe lack any musculature and therefore its homology remains uncertain. However, considering the potential contribution of the 'ligula' to the haustellum it cannot be excluded that this lobe indeed represents a remnant of the paraglossa.

The labial palp of Trichoptera is usually three-segmented (four-segmented only in *Paduniella* [Psychomyiidae]) in both sexes (Malicky 1973). In Lepidoptera it is three-segmented in some lower groups but reduction in number of palpomeres occurs several times within the group (Kristensen 2003).

4.1.14. Nervous system

In Trichoptera the cephalic ganglia (brain and suboesophageal ganglion; Fig. 18) are usually distinctly separated by long circumoesophageal connectives (in Hydroptilidae exceptionally short [Ehnbom 1948]). The brain is divided into a large dorsal protocerebrum, well-developed anterior olfactory lobes (deutocerebrum) and a small ventral tritocerebrum which is continuous with the other parts of the brain (pers. obs., Ehnbom 1948). Usually frontal and labral nerves have a common root at the frontal connectives and split later into separate frontal (median) and labral (lateral) tracts (pers. obs.; Ehnbom 1948). Only in Hydroptilidae and Lepidoptera both nerves show discrete origins (Ehnbom 1948). The nervous system of Hydroptilidae and Lepidoptera share also other remarkable similarities as for instance the penetration of the cephalic aorta by the nervus recurrens. Both structures are distinctly separated in all other trichopterans (Ehnbom 1948). The shape of the suboesophageal ganglion varies considerably among Trichoptera (Ehnbom 1948). Usually, three pairs of nerves (mandibular, maxillary and labial) origi-

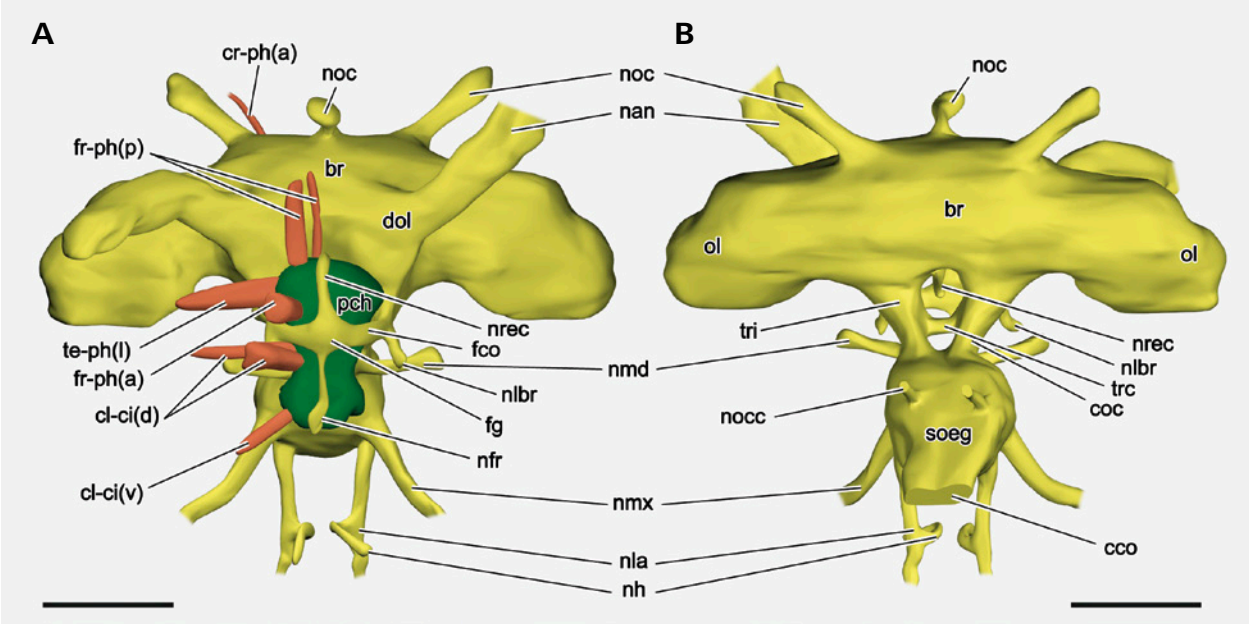

Fig. 18. *Philopotamus ludificatus* McLachlan, 1878: nervous system and gut with attached musculature (removed in B), 3D-reconstruction based on µCT data. **A**: anterior view, **B**: posterior view. — ***Colors***: green – gut, orange – musculature, yellow – nervous system. — ***Abbreviations***: br – brain, cco – cervical connective, cl-ci(d) – M. clypeo-cibarialis dorsalis, cl-ci(v) – M. clypeo-cibarialis ventralis, coc – circumoesophageal commissure, cr-ph(a) – M. cranio-pharyngalis anterior, dol – deutocerebral olfactory lobe, fco – frontal connective, fg – ganglion frontale, fr-ph(a) – M. fronto-pharyngalis anterior, fr-ph(p) – M. fronto-pharyngalis posterior, nan – nervus antennalis, nfr – nervus frontalis, nh – nerve of the haustellum, nla – labial nerve, nlbr – labral nerve, nmd – mandibular nerve, nmx – maxillary nerve, noc – ocellar nerve, nocc – occipital nerve, nrec – nervus recurrens, ol – optical lobe of protocerebrum, pch – precerebral pumping chamber, soeg – suboesophageal ganglion, te-ph(l) – M. tentorio-pharyngalis lateralis, trc – tritocerebral commissure, tri – tritocerebrum. (Scale bars: 250 µm)

nate ventrally in both, Trichoptera and Lepidoptera (EHNBOM 1948). An occipital nerve originating from the dorsal wall of the suboesophageal ganglion in *Philopotamus* is not described for any other trichopteran representative.

Paired glands of the hypocerebral complex, the corpora cardiaca and corpora allata are located behind the brain on both sides of the pharynx in Trichoptera and in Lepidoptera (EHNBOM 1948). However, comparative investigations showed considerable differences in shape and localization of the corpora cardiaca between different groups of caddisflies (EHNBOM 1948). In *Philopotamus* they are close to the hind face of the brain and ellipsoidally shaped as it is also described for *Hydropsyche* and *Agraylea* (Hydropsychidae, Hydroptilidae [EHNBOM 1948]). In Limnephilidae the corpora cardiaca are rather slender and distinctly separated from the brain (EHNBOM 1948). In *Philopotamus* the corpora allata are quite prominent (several times larger than the corpora cardiaca) and characterized by a considerably irregular glandular structure (pers. obs.; EHNBOM 1948). This condition is unique among trichopterans but resembles the condition found in most lepidopterans (EHNBOM 1948).

The cervical connectives are well separated from each other in Trichoptera and Mecoptera (*Panorpa* [EHNBOM 1948]). A different pattern is described for Hydroptilidae in which the cervical connectives being almost completely fused (EHNBOM 1948). This resembles the common condition in Lepidoptera excluding Micropterigidae (EHNBOM 1948).

4.2. Ground plan reconstruction

With this contribution to the soft-tissue anatomy of an annulipalpian species information for all three traditional trichopteran suborders is now available (Spicipalpia paraphyletic; see e.g., KJER et al. 2002; HOLZENTHAL et al. 2007b). Our data show remarkable intraordinal heterogeneity in several character complexes. As pointed out above, data are only available for few lineages (Rhyacophilidae, Philopotamidae, and Phryganeidae). This situation as well as the unresolved phylogeny of Trichoptera impedes a thorough interpretation of the structural evolution within Trichoptera. Nevertheless, the current state of knowledge allows us to hypothesize the trichopteran ground plan condition for several characters.

The tentorium of most Trichoptera is Π-shaped (NEBOISS 1991), a condition which can be interpreted as a plesiomorphic ground plan feature of the group (KRISTENSEN 2003). The X-shaped tentorium of Philopotamidae and Hydropsychidae most likely represents a derived condition in Trichoptera. Furthermore, a plate-like corpotentorium is only present in Philopotamidae (see also NEBOISS 1991) and most likely represents an autapomorphy of this annulipalpian lineage, which is paralleled in the non-glossatan Lepidoptera families Agathiphagidae and Heterobathmiidae (KRISTENSEN 2003). The dorsal tentorial arms are very short in Annulipalpia and some spicipalpian groups (Glossosomatidae and Hydroptilidae) (NEBOISS 1991). This configuration most likely represents

the ground plan condition of Amphiesmenoptera since the same condition is present in primitive non-glossatan Lepidoptera (see KRISTENSEN 2003). Considering this, the well-developed and sclerotized dorsal tentorial arms of the integripalpian lineage Plenitentoria (e.g., CRICHTON 1957) represent a derived condition and a potential autapomorphy of the group.

In the ground plan of Amphiesmenoptera (as in most other insects [WIPFLER et al. 2011]) the antenna is moved by four extrinsic muscles, primarily originating from the anterior tentorial arms. This pattern is retained in the ground plan of Trichoptera. However, shifts of the origin sites toward the head capsule occur in several taxa. These secondary modifications were found in distantly related taxa (e.g., Hydropsychidae [Annulipalpia] and Hydroptilidae ['Spicipalpia']) and are therefore regarded as independent developments (homoplasies). The shift of the origin of M. tentorio-scapalis posterior toward the dorsal tentorial arm in all studied species of Plenitentoria (pers. obs.; CRICHTON 1957) very likely represents a further autapomorphy of this group.

The adult mandibular sclerite in the ground plan of Trichoptera is moderately sized and sclerotized but it is certainly not suitable to process solid food (see above). This condition is retained in Annulipalpia and in the spicipalpian lineage Rhyacophilidae. The mandibular sclerite is extremely reduced in size and sclerotization in Integripalpia (see CRICHTON 1957), showing a distinct trend to the reduction of this chewing mouthpart within Trichoptera. We assume that the loss of the feeding function of the mandible is the reason for this reduction. While the evolution of the skeletal elements is clear, the correlated changes in the muscle system are ambiguous. Three well-developed pairs of muscles associated with the mandible can be assumed in the ground plan of Trichoptera. Beneath the large cranial adductor and abductor muscles, a thin tentorio-mandibular muscle is present in the spicipalpian (KLEMM 1966) and annulipalpian representatives investigated so far. The loss of this muscle in integripalpian representatives (e.g., *Limnephilus*, pers. obs.) can be interpreted as an apomorphy of Integripalpia or one of its subgroups. Otherwise it may be a result of independent reductions. This aspect cannot be reconstructed with the present data and should be investigated more thoroughly. The dimensions of the cranio-mandibular muscles are very heterogeneous. While for *Philopotamus* (see above) and *Rhyacophila* (KLEMM 1966) extensively sized muscles are reported, the musculature of phryganeid species is comparatively small and slender (CRICHTON 1957). Analog to the mandible itself, this could be interpreted as a trend to size-reduction in the evolution of Trichoptera. Interestingly, KLEMM (1966) did not find well-developed muscles in all specimens studied. Thus it is also possible that the recorded morphological differences are caused by individual muscle degenerations in the adult stage after eclosion in all caddisflies as proposed by HINTON (1946). Consequently, the reduction of these mandibular muscles should be interpreted as a ground plan feature of Trichoptera. The main drawback of all anatomical studies is the unknown age of the specimens caught in the wild. Further investigations on the development of the musculature from specimens of exactly defined age are needed to answer this question with quantitative data.

The morphology of the digestive tract and its associated musculature is quite uniform throughout Trichoptera. Differences occur only in the origin of the ventral cibarial dilators from below (Philopotamidae, Rhyacophilidae; pers. obs.; KLEMM 1966) or from above (Phryganeidae; CRICHTON 1957) the intraclypeal sulcus. The data at hand suggest that the origin below the intraclypeal sulcus is the plesiomorphic condition in Trichoptera but further comparative studies are necessary to homologize the clypeal dilators of the prepharyngeal tube and to trace their modifications during the evolution of the group.

The presence of a maxillary lobe comprising a large, chemoreceptive galea and a small median lacinia is part of the amphiesmenopteran ground plan (see also KRISTENSEN 2003). These features are widely retained in the trichopteran ground plan (present in Rhyacophilidae [KLEMM 1966] and Annulipalpia), except for the loss of a free, well-developed lacinia. A dististipital adductor originating from the anterior tentorial arm is present in almost all trichopteran lineages studied to date. As the muscle is regularly present in basal lepidopterans and other holometabolan insects (e.g., HANNEMANN 1956; FRIEDRICH et al. 2013; RANDOLF el al. 2014) its occurrence in Trichoptera is plesiomorphic. Its absence in Phryganeidae (Integripalpia; CRICHTON 1957) might be autapomorphic for this family. A stipito-lacinial flexor can also be assumed to be part of the ground plan of Amphiesmenoptera since it is well-developed in the non-glossatan moth lineage Micropterigidae (KRISTENSEN 2003) and in the majority of trichopteran lineages. The known exceptions are the annulipalpian families Hydropsychidae and Philopotamidae (pers. obs.). Due to absence of data it is not known if the loss of this muscle is an autapomorphy of the suborder.

The number of maxillary palpomeres in the ground plan of Amphiesmenoptera is five (see KRISTENSEN 2003) as it is in all Annulipalpia and 'Spicipalpia'. It is convergently reduced in males throughout Integripalpia (e.g., Plenitentoria: Limnephilidae, Phryganeidae, Brachycentridae; Brevitentoria: Sericostomatidae [MALICKY 1973, 2004]).

The composite haustellum represents the only unequivocal autapomorphy of Trichoptera (KRISTENSEN 1997). The surface structure, i.e., the arrangement of microtrichia, varies notably between the major trichopteran lineages (see e.g., KLEMM 1966; CRICHTON 1957). Representatives of Integripalpia and Rhyacophilidae exhibit longitudinal channels (KLEMM 1966; CRICHTON 1957), whereas the spicipalpian lineages Hydroptilidae and Glossosomatidae show a more transverse arrangement (KRISTENSEN 1997). The latter condition was interpreted as the ground plan condition of Trichoptera by KRISTENSEN (1997), because a very similar arrangement of spines was observed in the infrabuccal pouches of non-glossatan

moths. However, the condition of the annulipalpian haustellum does not fit well in this scenario. At the present state of knowledge it is uncertain if the annulipalpian small, granulose haustellum lost the channels secondarily (potential autapomorphy of Annulipalpia) or represents the plesiomorphic condition in Trichoptera. Detailed comparative studies on the haustellum, especially of the fine structure of the channels are needed to infer the homology of these structures in Amphiesmenoptera and to reconstruct the ground plan of Trichoptera.

The flexible roof of the salivarium, moved against the floor by a hypopharyngo-salivary dilator muscle, is usually present in all holometabolan lineages, where it originates from the hypopharynx (most Lepidoptera [Kristensen 2003], Neuroptera [Randolf et al. 2014], many dipterans [Schneeberg & Beutel 2011]) or from the ligula (Megaloptera; Röber 1942). Within Trichoptera this condition is only described for Philopotamidae, but represents a plesiomorphic ground plan feature of the order. It is unknown if this plesiomorphy is also retained in other annulipalpians. In other trichopteran lineages the origin site of the muscle is remarkably modified. It forms an intrasalivarial muscle running longitudinally along the roof of the salivarium in Integripalpia and Rhyacophilidae. A similar condition is also known from many mecopteran groups (e.g., Heddergott 1938; Grell 1938; Friedrich et al. 2013).

A further potential autapomorphy of Trichoptera is the insertion of the premental dilator muscle dorsally on the roof of the salivarium (Fig. 16E,F; Klemm 1966: 2s). The usual attachment sites of this muscle in other holometabolan insects (e.g., Neuropterida [Röber 1942; Randolf et al. 2014]; Hymenoptera [Vilhelmsen 1996]) are the lateral wall or the floor of the salivarium. As the muscle is absent in Lepidoptera (Kristensen 2003) it cannot be assigned to the ground plan of Amphiesmenoptera.

The paired endite lobes of the labium are distinctly developed in Annulipalpia (e.g., Fig. 7F) and Rhyacophilidae (Klemm 1966). Even though the homology to the lepidopteran paraglossa or ligula (Kristensen 2003) remains unclear (see above), the appendages certainly represent a trichopteran ground plan feature. In contrast, the loss of endite lobes in integripalpian lineages is the derived condition and maybe an apomorphy of the suborder.

As pointed out earlier only the evolution of some features of the adult head in Trichoptera can be reconstructed with the data at hand. The lack of comparative data for the majority of families renders the reconstruction of evolutionary scenarios for the suborders almost impossible. Furthermore, the assignment of anatomical features to the trichopteran ground plan is strongly hampered by the unresolved placement of the 'spicipalpian' families. Additionally, detailed and comprehensive information on internal morphology is also needed for the non-cephalic tagmata of adults and other life stages. The anatomy of an extensive number of trichopteran lineages should be investigated to infer the phylogenetic relationship of the order based on morphological characters, to test phylogenies from molecular data, and to trace the evolution of major morphological and behavioral traits within the order.

5. Acknowledgements

We are very grateful to Univ.-Prof. Dr. Hans Malicky (Lunz am See, Austria) for his help during the collecting of *P. ludificatus* and also for providing additional material from his valuable collection. Prof. Dr. Niels Peder Kristensen (University of Copenhagen) helped to improve the manuscript during numerous fruitful discussions about the morphology of Amphiesmenoptera. His outstanding contribution is greatly acknowledged. Furthermore, we thank Dr. Klaus-Dieter Klass (Senckenberg Naturhistorische Sammlungen Dresden), Dr. Benjamin Wipfler (University of Jena) and one anonymous reviewer for helpful comments which greatly improved the manuscript. We thank Rommy Petersohn (University of Jena) for the preparation of histological section series. Renate Walter (University of Hamburg) prepared SEM samples and helped us with the digitalization of histological section series. This is also greatly acknowledged. We thank the DESY facility, Hamburg (project number: I-20100317) for the possibility to obtain high quality SR-µCT-data at storage ring DORIS III. We thank Prof. Dr. Rolf G. Beutel (University of Jena) for offering us the opportunity to use Bitplane Imaris software in his lab. A research stay of MK in Copenhagen was supported by a grant from the European Commission's (FP 7) Integrated Infrastructure Initiative programme SYNTHESYS (DK-TAF-4052) which is kindly appreciated. The financial support for the project provided by the Deutsche Forschungsgemeinschaft (DFG) (FR 3062/2-1) is greatly acknowledged. The support of Dr. Ralph S. Peters (Forschungsmuseum A. Koenig, Bonn) in this matter is also acknowledged.

6. References

Beckmann F., Donath T., Fischer J., Dose T., Lippmann T., Lottermoser L., Martins R.V., Schreyer A. 2006. New developments for synchrotron-radiation-based microtomography at DESY. – Proceedings of SPIE **6318**: 1–10.

Beckmann F., Herzen J., Haibel A., Müller B., Schreyer A. 2008. High density resolution in synchrotron-radiation-based attenuation-contrast microtomography. – Proceedings of SPIE **7078**: D–1–10.

Bernhard C.G., Gemne G., Sällström J. 1970. Comparative ultrastructure of corneal surface topography in insects with aspects on phylogenesis and function. – Zeitschrift für Vergleichende Physiologie **67**: 1–25.

Bernhard C.G., Miller W.H. 1962. A corneal nipple pattern in insect compound eyes. – Acta Physiologica Scandinavica **56** (3–4): 385–386.

Beutel R.G., Friedrich F., Ge S.-Q., Yang X.-K. 2014. Insect Morphology and Phylogeny. A textbook for students of entomology. – Walter de Gruyter, Berlin, Boston. 516 pp.

Beutel R.G., Friedrich F., Hörnschemeyer T., Pohl H., Hünefeld F., Beckmann F., Meier R., Misof B., Whiting M.F., Vilhelmsen L. 2011. Morphological and molecular evidence converging upon a robust phylogeny of the megadiverse Holometabola. – Cladistics **27**(4): 341–355.

Chamorro M.L., Holzenthal R.W. 2011. Phylogeny of Polycentropodidae Ulmer, 1903 (Trichoptera: Annulipalpia: Psychomyioidea) inferred from larval, pupal and adult characters. – Invertebrate Systematics **25**: 219–253.

Chaudonneret J. 1990. Les Pièces Buccales des Insectes. Thème et Variations. – Édition hors Série du Bulletin Scientifique de Bourgogne. 255 pp.

Crichton M.I. 1957. The structure and function of the mouth parts of adult caddis flies (Trichoptera). – Philosophical Transactions of the Royal Society B **241**: 45–91.

Crichton M.I. 1989. A scanning electron microscope study of the mouth parts of adult *Phryganea grandis* (L.) (Trichoptera). Pp. 329–333 in: Tomaszewski C. (ed.), Proceedings of the 6th International Symposium on Trichoptera. – Adam Mickiewicz Press, Poznan.

Crichton M.I. 1992. A scanning electron microscope study of the mouth parts of some adult Limnephilidae (Trichoptera). Pp. 45–48 in: Otto C. (ed.), Proceedings of the 7th International Symposium on Trichoptera. – Backhuys Publishers, Leiden.

Cummings B.F. 1914. Note on the characters of the head and mouthparts in the genera *Plectrotarsus* and *Æthaloptera* (Trichoptera). – Annals and Magazine of Natural History **14**(8): 22–31.

Demoulin G. 1960. Quelques remarques sur la composition segmentaire de la tete des Insectes. Part I: Variations de la capsule céphalique de la larve à l'adulte, chez quelques insectes mécoptéroides. – Bulletin Institut Royal des Sciences Naturelles de Belgique **36**(18): 1–12.

Denis J.R., Bitsch J. 1973. Morphologie de la tête des insectes. In: Grassé P.P. (ed.), Traité de Zoologie VIII(1). – Masson et Cie, Paris. 593 pp.

Deoras P.J. 1943. On the comparative morphology and evolution of adult Trichoptera. Part I: External morphology. – Indian Journal of Entomology **5**: 177–188.

Despax R. 1951. Ordre des Trichoptères. In: Grassé P.P. (ed.), Traité de Zoologie X(1). – Masson et Cie, Paris. pp. 125–173.

Drilling K., Klass K.-D. 2010. Surface structures of the antenna of Mantophasmatodea (Insecta). – Zoologischer Anzeiger **249**: 121–137.

Ehnbom K. 1948. Studies on the central and sympathetic nervous system and some sense organs in the head of neuropteroid insects. – Opuscula Entomologica Supplementum **8**: 1–162.

Faucheux M.J. 2004. Antennal sensilla of Trichoptera and Lepidoptera: Phylogenetic considerations. – Bulletin de l'Institut Royal des Sciences Naturelles de Belgique, Entomologie **74**: 69–71.

Frania H.E., Wiggins G.B. 1997. Analysis of morphological and behavioural evidence for the phylogeny and higher classification of Trichoptera (Insecta). – Royal Ontario Museum Life Sciences Contributions **160**: 1–67.

Friedrich F., Beutel R.G. 2010. Goodbye Halteria? The thoracic morphology of Endopterygota (Insecta) and its phylogenetic implications. – Cladistics **26**(6): 579–612.

Friedrich F., Pohl H., Beckmann F., Beutel R.G. 2013. The head of *Merope tuber* (Meropeidae) and the phylogeny of Mecoptera (Hexapoda). – Arthropod Structure & Development **42**(1): 69–88.

Friedrich F., Matsumura Y., Pohl H., Bai M., Hörnschemeyer T., Beutel R.G. 2014. Insect morphology in the age of phylogenomics: innovative techniques and its future role in systematics. – Entomological Science **17**(1): 1–24.

Grell K.G. 1938. Der Darmtraktus von *Panorpa communis* L. und seine Anhänge bei Larve und Imago (Ein Beitrag zur Anatomie und Histologie der Mecopteren). – Zoologische Jahrbücher, Abteilung für Anatomie und Ontogenie der Tiere **64**: 1–86.

Hagberg M. 1986. Ultrastructure and central projections of extraocular photoreceptors in caddisflies (Insecta: Trichoptera). – Cell and Tissue Research **245**: 643–648.

Hallberg E., Hagberg M. 1986. Ocellar fine structure in *Caenis robusta* (*Ephemeroptera*), *Trichostegia minor*, *Agrypnia varia*, and *Limnephilus flavicornis* (*Trichoptera*). – Protoplasma **135**: 12–18.

Handlirsch A., Beier M. 1936. Trichoptera oder Köcherfliegen. Pp. 1491−1548 in: Kükenthal W., Krumbach T. (eds), Handbuch der Zoologie IV. Band: Arthropoda – 2. Hälfte: Insecta. 2. Teil: Spezielles. – Walter de Gruyter, Berlin, New York.

Hannemann H.J. 1956. Die Kopfmuskulatur von *Micropteryx calthella* L. (Lep.). Morphologie und Funktion. − Zoologische Jahrbücher, Abteilung für Anatomie und Ontogenie der Tiere **75**: 177–206.

Heddergott H. 1938. Kopf und Vorderdarm von *Panorpa communis* L. – Zoologische Jahrbücher, Abteilung für Anatomie und Ontogenie der Tiere **65**: 229−294.

Hinton H.E. 1946. A new classification of insect pupae. − Journal of Zoology **116**(2): 282−328.

Hinton H.E. 1958. The phylogeny of the panorpoid orders. – Annual Review of Entomology **3**: 118−206.

Holzenthal R.W., Blahnik R.J., Prather A.L., Kjer K.M. 2007a. Order Trichoptera Kirby, 1813 (Insecta), Caddisflies. – Zootaxa **1668**: 639–698.

Holzenthal R.W., Blahnik R.J., Kjer K.M., Prather A.P. 2007b. An update on the phylogeny of caddisflies (Trichoptera). Pp. 143–153 in: Bueno-Soria J., Barba-Alvarez R., Armitage B. (eds), Proceedings of the 12th International Symposium on Trichoptera. – The Caddis Press, Columbus, Ohio.

Holzenthal R.W., Morse J.C., Kjer K.M. 2011. Order Trichoptera Kirby, 1813. In: Zhang Z.-Q. (ed.), Animal biodiversity: An outline of higher-level classification and survey of taxonomic richness. – Zootaxa **3148**: 209–211.

Ivanov V.D. 1997. Rhyacophiloidea: a paraphyletic taxon. Pp. 189–193 in: Holzenthal R.W., Flint Jr. O.S. (eds), Proceedings of the 8th International Symposium on Trichoptera. – Ohio Biological Survey, Columbus, Ohio.

Kéler S. von 1955. Entomologisches Wörterbuch mit besonderer Berücksichtigung der morphologischen Terminologie. – Akademie-Verlag, Berlin. 679 pp.

Kjer K.M., Blahnik R.J., Holzenthal R.W. 2002. Phylogeny of caddisflies (Insecta, Trichoptera). – Zoologica Scripta **31**: 83–91.

Klass K.-D., Eulitz U. 2007. The tentorium and anterior head sulci in Dictyoptera and Mantophasmatodea (Insecta). – Zoologischer Anzeiger **246**: 205–234.

Klemm N. 1966. Die Morphologie des Kopfes von *Rhyacophila* Pict. (Trichoptera). – Zoologische Jahrbücher, Abteilung für Anatomie und Ontogenie der Tiere **83**: 1–51.

KRISTENSEN N.P. 1997. Early evolution of the Lepidoptera + Trichoptera lineage: phylogeny and the ecological scenario. In: GRANDCOLAS P. (ed.), The Origin of Biodiversity in Insects: Phylogenetic Tests of Evolutionary Scenarios. – Mémoires du Muséum National d'Histoire Naturelle **173**: 253–271.

KRISTENSEN N.P. 2003. Skeleton and muscles: adults. Pp. 39–131 in: KRISTENSEN N.P. (volume ed.), Handbuch der Zoologie. Band IV: Arthropoda: Insecta. Teilband 36: Lepidoptera, Moths and Butterflies. Volume 2: Morphology, Physiology, and Development. – Walter de Gruyter, Berlin, New York. 564 pp.

KRISTENSEN N.P., NIELSEN E.S. 1979. A new subfamily of micropterigid moths from South America. A contribution to the morphology and phylogeny of the Micropterigidae, with a generic catalogue of the family (Lepidoptera: Zeugloptera). – Steenstrupia **5**(7): 69–147.

LUCAS R. 1893. Beiträge zur Kenntnis der Mundwerkzeuge der Trichoptera. – Archiv für Naturgeschichte **59**: 285–330.

MALICKY H. 1973. Trichoptera (Köcherfliegen). In: HELMCKE J.-G., STARCK D., WERMUTH H. (eds), Handbuch der Zoologie. IV. Band: Arthropoda – 2. Hälfte: Insecta. 2. Teil: Spezielles. – Walter de Gruyter, Berlin, New York. 114 pp.

MALICKY H. 2001. Notes on the taxonomy of *Rhadicoleptus*, *Ptilocepus* and *Pseudoneureclipsis*. – Braueria **28**: 19–20.

MALICKY H. 2004. Atlas der Europäischen Köcherfliegen. Second Edition. – Springer Verlag, Dordrecht. 359 pp.

MALICKY H. 2005. Ein kommentiertes Verzeichnis der Köcherfliegen (Trichoptera) Europas und des Mediterrangebietes. – Linzer Biologische Beiträge **37**(1): 533–596.

MALM T., JOHANSON K.A., WAHLBERG N. 2013. The evolutionary history of Trichoptera (Insecta): A case of successful adaptation to life in freshwater. – Systematic Entomology **38**(3): 459–473.

MATSUDA R. 1965. Morphology and evolution of the insect head. – Memoirs of the American Entomological Institute **4**: 1–240.

MELNITSKY S.I., IVANOV V.D. 2011. Structure and localization of sensilla on antennae of caddisflies (Insecta: Trichoptera). – Journal of Evolutionary Biochemistry and Physiology **47**(6): 593–602.

MEYER-ROCHOW V.B., STRINGER I. 1993. A system of regular ridges instead of nipples on a compound eye that has to operate near the diffraction limit. – Vision Research **33**(18): 2645–2647.

MICKOLEIT G. 1971. Das Exoskelett von *Notiothauma reedi* Mac Lachlan, ein Beitrag zur Morphologie und Phylogenie der Mecoptera (Insecta). – Zeitschrift für Morphologie der Tiere **69**: 318–362.

MOULINS M. 1971. La cavité préorale de *Blabera craniifer* Burm. (Insecte, Dictyoptère) et son innervation: Etude anatomo-histologique de l'epipharynx et l'hypopharynx. – Zoologische Jahrbücher, Abteilung für Anatomie und Ontogenie der Tiere **88**(4): 527–586.

NEBOISS A. 1991. Comparative study of tentorial structures in caddis-flies (Trichoptera). Pp. 283–290 in: TOMASZEWSKI C. (ed.), Proceedings of the 6th International Symposium on Trichoptera. – Adam Mickiewicz University Press, Poznań.

NIELSEN E.S., KRISTENSEN N.P. 1996. The Australian moth family Lophocoronidae and the basal phylogeny of the Lepidoptera-Glossata. – Invertebrate Taxonomy **10**: 1199–1302.

OLÁH J., JOHANSON K.A. 2007. Trinominal terminology for cephalic setose warts in Trichoptera (Insecta). – Braueria **34**: 43–50.

PETERS R.S., MEUSEMANN K., PETERSEN M., MAYER C., WILBRANDT J., ZIESMANN T., DONATH A., KJER K.M., ASPÖCK U., ASPÖCK H., ABERER A., STAMATAKIS A., FRIEDRICH F., HÜNEFELD F., NIEHUIS O., BEUTEL R.G., MISOF B. 2014. The evolutionary history of holometabolous insects inferred from transcriptome-based phylogeny and comprehensive morphological data. – BMC Evolutionary Biology **14**: 52.

POHL H. 2010. A scanning electron microscopy specimen holder for viewing different angles of a single specimen. – Microscopy Research and Technique **73**: 1073–1076.

RANDOLF S., ZIMMERMANN D., ASPÖCK U. 2014. Head anatomy of adult *Nevrorthus apatelios* and basal splitting events in Neuroptera (Neuroptera: Nevrorthidae). – Arthropod Systematics and Phylogeny **72**(2): 111−136.

ROSS H.H. 1956. Evolution and Classification of the Mountain Caddisflies. – The University of Illinois Press, Urbana. 213 pp.

RÖBER H. 1942. Morphologie des Kopfes und des Vorderdarmes der Larve und Imago von *Sialis flavilatera*. – Zoologische Jahrbücher, Abteilung für Anatomie und Ontogenie der Tiere **67**: 61−118.

SCHMID F. 1989. Les Hydrobiosides (Trichoptera, Annulipalpia). – Bulletin de l'Institut Royal des Sciences Naturelles de Belgique, Entomologie **59** Supplement: 154 pp.

SCHMID F. 1998. Genera of the Trichoptera of Canada and adjoining or adjacent United States. In: HAYNES R.H. (ed.), The Insects and Arachnids of Canada. Part 7. – NRC Research Press, Ottawa. 319 pp.

SCHNEEBERG K., BEUTEL R.G. 2011. The adult head structures of Tipulomorpha (Diptera, Insecta) and their phylogenetic implications. – Acta Zoologica **92**: 316–343.

SNODGRASS R.E. 1935. Principles of Insect Morphology. – McGraw-Hill Book Company, New York, London. 667 pp.

SNODGRASS R.E. 1963. A contribution toward an encyclopedia of insect anatomy. – Smithsonian Miscellaneous Collections **146**: 1–48.

TILLYARD R.J. 1923. On the mouth parts of the Micropterygoidea (Lep.). – Transactions of the Entomological Society of London 1923: 181–206.

VILHELMSEN L. 1996. The preoral cavity of lower Hymenoptera (Insecta): comparative morphology and phylogenetic significance. – Zoologica Scripta **25**(2): 143–170.

WEAVER III J.S. 1984. The evolution and classification of Trichoptera, Part I: The ground plan of Trichoptera. Pp. 413−419 in: MORSE J.C. (ed.), Proceedings of the 4th International Symposium on Trichoptera. – Dr. W. Junk Publishers, The Hague, Boston, Lancaster.

WIPFLER B., MACHIDA R., MÜLLER B., BEUTEL R.G. 2011. On the head morphology of Grylloblattodea (Insecta) and the systematic position of the order, with a new nomenclature for the head muscles of Dicondylia. – Systematic Entomology **36**(2): 241–266.

WIGGINS G.B., WICHARD W. 1989. Phylogeny of pupation in Trichoptera, with proposals on the origin and higher classification of the order. – Journal of the North American Benthological Society **8**: 260–276.